Cellular Mechanism of Obsessive-Compulsive Disorder

by

Louis Yunshou Tee

Department of Neurobiology
Duke University

Date:_____
Approved:

_____
Guoping Feng, Co-Supervisor

_____
Dona Chikaraishi, Co-Supervisor

_____
Fan Wang

_____
Anne West

Dissertation submitted in partial fulfillment of
the requirements for the degree of Doctor of Philosophy in the Department of
Neurobiology in the Graduate School
of Duke University

2015

ABSTRACT

Cellular Mechanism of Obsessive-Compulsive Disorder

by

Louis Yunshou Tee

Department of Neurobiology
Duke University

Date:_____
Approved:

_____
Guoping Feng, Co-Supervisor

_____
Dona Chikaraishi, Co-Supervisor

_____
Fan Wang

_____
Anne West

An abstract of a dissertation submitted in partial
fulfillment of the requirements for the degree
of Doctor of Philosophy in the Department of
Neurobiology in the Graduate School of
Duke University

2015

# Abstract

Obsessive-compulsive disorder (OCD) is a devastating illness that afflicts around 2% of the world's population with recurrent distressing thoughts (obsessions) and repetitive ritualistic behaviors (compulsions). While dysfunction at excitatory glutaminergic excitatory synapses leading to hyperactivity of the orbitofrontal cortex and head of the caudate – brain regions involved in reinforcement learning – are implicated in the pathology of OCD, clinical studies in patients are unable to dissect the molecular mechanisms underlying this cortico-striatal circuitry defect. Since OCD is highly heritable, recent studies using mutant mouse models have shed light on the cellular pathology mediating OCD symptoms. These studies point toward a crucial role for ΔFosB, a persistent transcription factor that accumulates with chronic neuronal activity and is involved in various diseases of the striatum. Furthermore, elevated ΔFosB levels results in the transcriptional upregulation of *Grin2b*, which codes GluN2B, an *N*-methyl-D-aspartate glutamate receptor (NMDAR) subunit required for the formation and maintenance of silent synapses. Taken together, the current evidence indicates that ΔFosB-mediated expression of aberrant silent synapses in caudate medium spiny neurons (MSNs), in particular D1 dopamine-receptor expressing MSNs (D1 MSNs), mediates the defective cortico-striatal synaptic transmission that underlies compulsive behavior in OCD.

# Dedication

To my family and friends for their invaluable encouragement and support

# Contents

# List of Tables

# List of Figures

## Acknowledgements

I thank my thesis committee – Professors Guoping Feng, Dona Chikaraishi, Fan Wang and Anne West – for their discerning advice, and members of the Feng lab for their patient instruction and insightful discussions. I especially thank Marie-Sophie van der Goes, Jin-ah Kim and Zhanyan Fu for their tireless and collegial collaboration, without which this project would not have been completed. Likewise, Sarah Schneck, Triana Dalia and Chunxia Li have provided excellent technical assistance during my graduate career. My graduate program is funded by an MD-PhD scholarship from the Agency for Science, Technology and Research in Singapore and the McGovern Institute for Brain Research at the Massachusetts Institute of Technology.

# Chapter 1: Introduction

At any given time, 1 to 3% of the world's population suffers from the debilitating obsessions and compulsions that define obsessive-compulsive disorder (OCD) (Kessler, 2005). While hyperactivity of the orbitofrontal cortex, head of the caudate and thalamus have been implicated in OCD, the specific cellular and synaptic pathologies mediating this increased brain activity has only recently been elucidated using mouse models of the disease. These recent advances promise to uncover new avenues for the understanding and treatment of OCD and OC-spectrum disorders.

## *1.1 Clinical studies in OCD patients*

Clinical studies have indicated that defects in neurotransmission in the cortico-striato-thalamo-cortical circuitry underlies OCD symptoms. Epidemiological studies have shown significant heritability of OCD, suggestive of heterogeneous genetic etiologies converging onto similar OCD symptoms (Nestadt, 2010; Bienvenu, 2000). Moreover, genome-wide association studies (GWAS) have identified numerous candidate genes that are involved in glutaminergic neurotransmission, suggesting a defect in glutaminergic signaling in OCD. Imaging, neurosurgical and epidemiological investigations involving patients suffering from OCD have also uncovered important clues to the neurobiological basis of this illness. Neuroimaging and neurosurgical studies have consistently implicated cortico-striato-thalamo-cortical circuitry hyperactivity in obsessions and compulsions, and abnormal cortico-striatal activity can be normalized of by proven therapies for OCD: cognitive behavioral therapy (CBT), pharmacotherapy and deep brain stimulation (Harrison, 2009; Menzies, 2008; Greenburg, 2006; Pauls, 2014).

### 1.1.1 Genetic epidemiology

Familial and twin studies have shown significant heritability of OCD, suggestive of a strong genetic component in the disease (Nestadt, 2010). 21% of the siblings and 37% of the parents of OCD patients also suffer from the illness, and first-degree relatives

of patients with OCD have around a five-fold higher risk of having the disease (10%) compared to normal controls (1.9%) (Nestadt, 2000; Hasler, 2007) . Similarly, twin studies show a higher concordance in monozygotic twins (87%) compared to dizygotic twins (49%) (Carey, 1981). Correspondingly, segregation analyses of OCD have rejected sporadic and environmental models for the etiology of OCD, and support a genetic basis for the disease (Nestadt, 2000).

Genome-wide linkage studies and genome-wide association studies (GWAS) have associated some genetic loci and single nucleotide polymorphisms (SNPs) with OCD. The largest linkage study conducted so far, the OCD Collaborative Genetics Study (OCGS), scanned the genomes of 1,008 subjects from 219 families using 386 microsatellite markers spaced an average of 9 centiMorgans apart. The study identified two putative linkage regions on chromosome 1(p=0.003) and chromosome 3 (p=0.0002) (Samuels, 2006).

In addition, two genome-wide association studies (GWAS) of OCD have been conducted (Steward, 2013; Mattheisen, 2014). The first GWAS, by the OCD Foundation Genetics Collaborative, examined 469,410 autosomal and 9,657 X-chromosomal SNPs from 1,465 patients, 5,557 controls and 400 trios (affected patients and parents), while the second study, by the OCD Collaborative Genetics Association Study (OCGAS), investigated 549,123 autosomal SNPs from 1,065 families and 1,406 cases. The two studies have two candidate genes in common: DLGAP1, a post-synaptic scaffolding

protein at glutaminergic excitatory synapses, and GRIK2, a subunit of the glutaminergic kainite receptor. In addition, many of the candidate genes identified from the two GWAS are associated with glutaminergic signaling.

**Table 1: Candidate genes from genome-wide association studies of OCD**

| Gene | Function of protein encoded by gene | P value |
|---|---|---|
| DLGAP1 | Post-synaptic density scaffolding protein in excitatory glutaminergic synapses<br>Isoform of DLGAP3 (also known as *Sapap3*) | 2 SNPs<br>$P=2.49x10^{-6}$<br>$P= 3.44x10^{-6}$ |
| BTBD3 | Transcription factor that regulates expression of genes involved in glutaminergic transmission such as GRIK1, GRIK4, DLGAP3, SHANK3 and ADARB2 | $P=3.84x10^{-8}$ |
| PTPRD | Presynaptic tyrosine phosphatase receptor that promotes maturation of glutaminergic synapses and neurite outgrowth<br>Binds to SLITRK postsynaptic adhesion molecules | $P=4.13x10^{-7}$ |
| GRIK2 | Subunit of post-synaptic glutaminergic kainite receptor (GluK2) | 2 SNPs<br>$P=2.96x10^{-6}$<br>$P=8.52x10^{-6}$ |
| FAIM2 | Involved in FAS-mediated cell death<br>Colocalizes with GluA2 glutamate receptor subunit | $P=4.99x10^{-7}$ |

Indeed, aberrant glutaminergic signaling at excitatory synapses is proposed to underlie OCD symptoms (Pittenger, 2011). In addition to the results of the two GWAS, genetic studies in human patients have revealed higher frequencies of polymorphisms of the GLUN2B gene at the three prime untranslated region (3'-UTR), a region that regulates mRNA transcript translation and stability (Arnold, 2004; Alonso, 2012; Arnold,

2009). GluN2B is crucial for the formation of $\alpha$-amino-3-hydroxy-5-methyl-4-isoxazolepropionic acid glutamate receptor (AMPAR)-silent synapses, and GluN2B signaling inhibits the insertion of AMPARs to silent synapses to unsilence them (Hanse, 2013; Hall, 2007). Similarly, linkage studies have implicated SLC1A1, which encodes for EAAC1 (Grados, 2010; Arnold, 2006), a glutamate transporter that limits the activation of perisynaptic GluN2B-containing NMDARs (Scimemi, 2009).

Furthermore, exon and intron-exon junction sequencing of samples from OCD patients with trichotillomania have uncovered missense mutations and single nucleotide polymorphisms (SNPs) in DLGAP3 (also known as *Sapap3*). DLGAP3 is an isoform of DLGAP1, a candidate gene identified in both OCD GWAS. The *Sapap* family of genes encodes for a scaffolding protein in the post-synaptic density of excitatory glutaminergic synapses that orchestrates homeostatic scaling of excitatory synapses (Zuchner, 2009; Bienvenu, 2009; Boardman, 2011; Romorini, 2004; Sheng, 2007).

*Sapap3*-null mice, which exhibit compulsive grooming behavior that responds to fluoxetine treatment, have elevated GluN2B levels in the post-synaptic density (Welch, 2007), and pharmacological antagonism of GluN2B alleviates compulsive grooming in these mice. Correspondingly, preliminary studies using NMDAR antagonists such as memantine and ketamine have been able to reduce obsessions and compulsions in OCD patients (Stewart, 2010; Aboujaoude, 2009; Rodriguez, 2011; Bloch, 2012). Therefore, it is

likely that unregulated NMDAR activity at excitatory glutaminergic synapses mediates the aberrant cortico-striatal synaptic transmission in OCD.

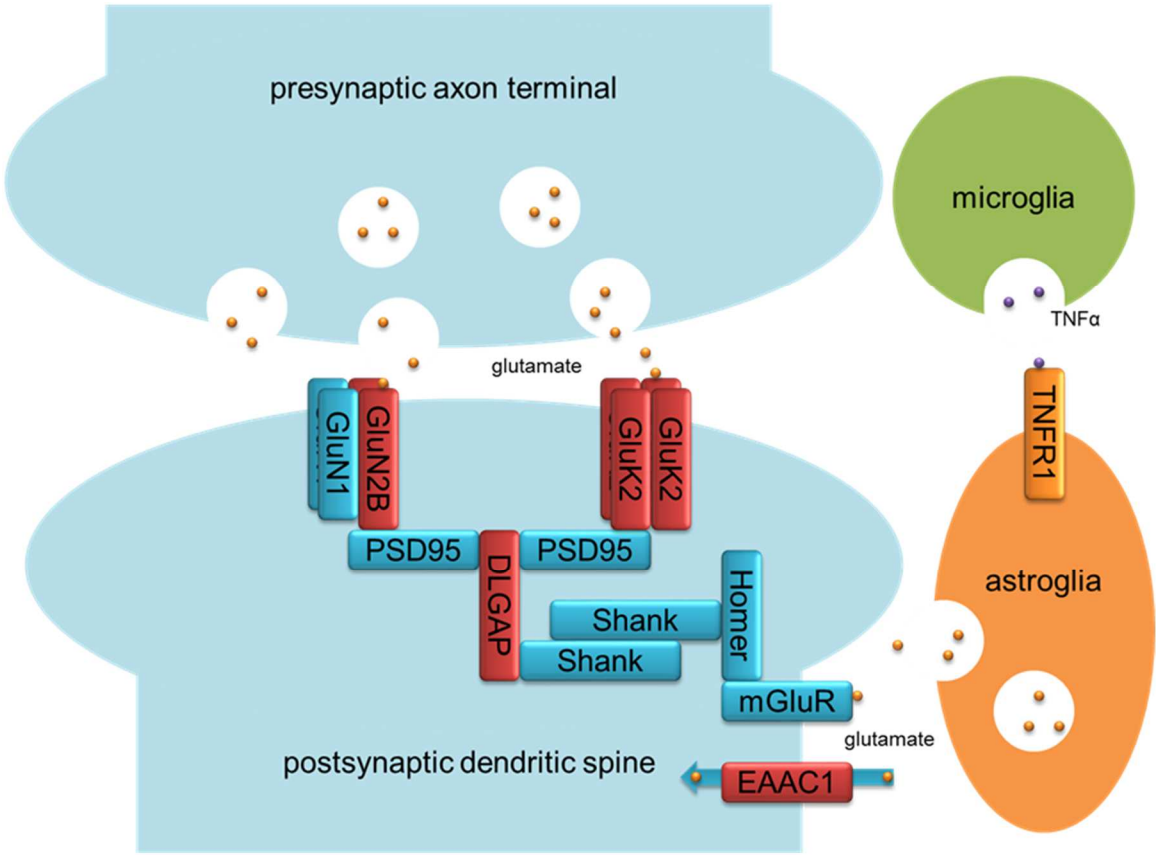


**Figure 1: Selected proteins implicated in OCD at the glutaminergic synapse**

### 1.1.2 Cortico-striatal-thalamo-cortical circuit defect

Neuroimaging studies in patients of OCD have reliably observed a cortico-striatal-thalamo-striatal (CSTC) circuitry defect. Positron emission tomography (PET) scans have showed increased glucose metabolism in the cerebral hemispheres, orbital

gyri and head of the caudate nucleus in OCD patients in both resting and provocation studies (Menzies, 2008). Furthermore, functional magnetic resonance imaging (fMRI) studies have demonstrated abnormal connectivity between the orbitofrontal cortex and striatum in subjects with OCD, and the strength of connectivity correlates with symptom severity (Sakai Y., 2011).

Neurosurgery in patients with OCD refractory to pharmacotherapy and psychotherapy have strengthened the hypothesis that the cortico-striato-thalamo-cortical circuitry is dysfunctional in OCD. For instance, anterior capsulotomy, the severing of white matter tracts connecting the cortex and thalamus with the striatum, reduces OCD symptoms in refractory OCD (Greenburg, 2006). Furthermore, deep brain stimulation (DBS) at the internal capsule, axon tracts linking cortical and thalamic projection neurons with the striatum, normalizes the altered fronto-striatal connectivity in patients and alleviates OCD symptoms (Denys, 2010; Greenburg, 2006; Figee, 2013). Therefore, both neuroimaging and neurosurgical studies have suggested that a cortico-striatal-thalamo-cortical circuitry defect mediates OCD symptoms.

A limitation of imaging studies is the inability to attain cellular resolution and to distinguish between excitation and inhibition of brain regions (Logothetis, 2008; Logothetis, 2001). Dissection of activity at the cellular level is required for dissecting the two opposing pathways in the cortico-striatal-thalamo-cortical circuit, the direct and indirect pathways. The direct pathway consists of medium spiny neurons in the

striatum that express Gs-coupled dopamine 1a receptors (D1 MSNs), and these neurons project to the globus pallidus interna (GPi) to activate the cortico-striatal-thalamo-cortical ciruitry (Kreitzer, 2009). On the other hand, the indirect pathway consists of medium spiny neurons (D2 MSNs) that inhibit the cortico-striatal-thalamo-cortical loop. These neurons express Gi-coupled dopamine 2 receptors, and project to the globus pallidus externa (GPe) (Kreitzer, 2009). D1 and D2 MSNs are intermingled and morphologically indistinguishable, making dissection of the direct and indirect pathways challenging in imaging studies.

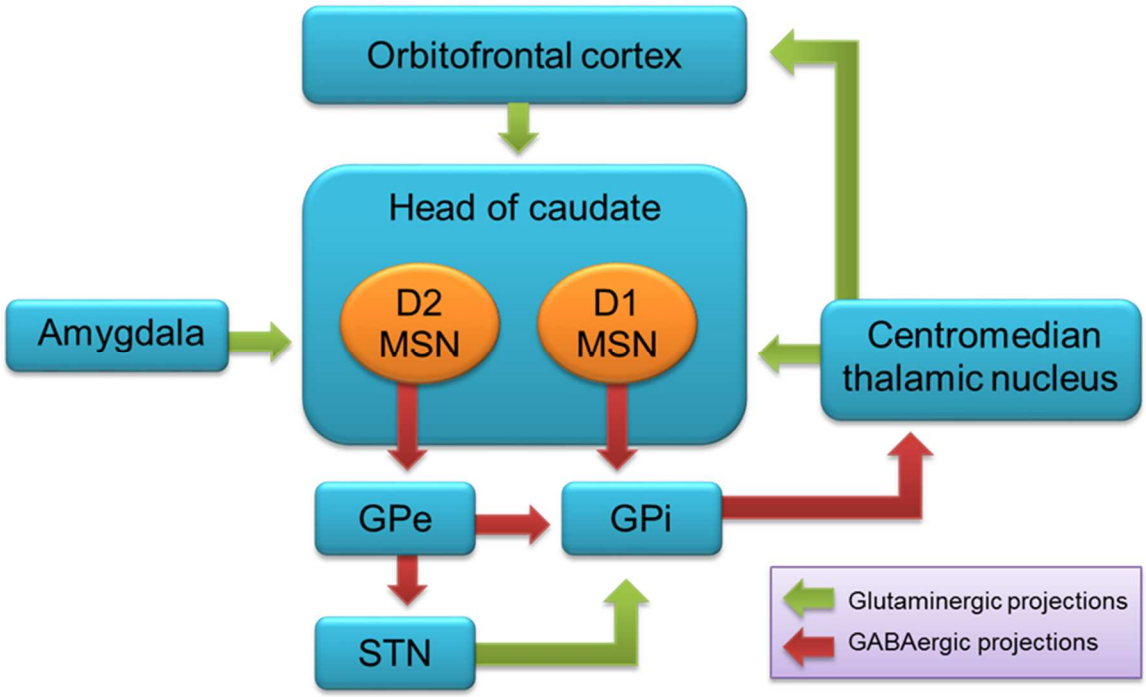


**Figure 2: Circuitry of brain regions involved in obsessive-compulsive disorder**

The cortico-striatal-thalamo-cortical circuitry is involved in motor control, acquisition of action-outcome associations, reinforcement learning, and motivation. The putamen, which receives inputs from the motor cortex, controls movements: D1 MSNs promote movement while D2 MSNs inhibit it (Hanse, 2013). Likewise, the limbic cortex (including the cingulate cortex) projects to the nucleus accumbens, to promote appetitive behaviors when D1 MSNs are activated, or aversive behaviors when D2 MSNs are activated (Hikida, 2010; Haber S.N., 1995; Lu X.Y., 1998; Richard, 2011). Increased activation of D1 MSNs in the nucleus accumbens results in compulsive drug seeking in cocaine addiction (Everitt, 2005), while inadequate D1 MSN activity can cause the learned helplessness in major depressive disorder (Vialou, 2010). Finally, the frontal cortex, which connects with the caudate, is involved in the acquisition of action-outcome associations (Hare, 2008). In particular, the orbitofrontal cortex projects to the head of the caudate to regulate reinforcement learning (Wilson, 2013), and compulsive behavior seen in OCD can result when D1 MSNs of the head of the caudate are aberrantly active (Graybiel, 2000). Furthermore, dopamine modulates in the two pathways differently. Basal, tonic dopamine levels activate high-affinity D2 receptors in D2 MSNs to inhibit the indirect pathway, whereas high, phasic dopamine levels – released in response to highly novel, rewarding or aversive stimuli – stimulate low-affinity D1 receptors in D1 MSNs to activate the direct pathway (Glimcher, 2011). Evidence from mouse models of

OCD suggest that an imbalance of the direct and indirect pathways of the cortico-striatal-thalamo-cortical circuitry mediates the symptoms of OCD.

The various cortico-striatal-thalamo-cortical circuits controlling motivation, reinforcement learning and movement can modulate one another, and the striatum also receive inputs from external structures such as the amygdala and hippocampus (Thorn, 2010; Voom, 2004). During reinforcement learning, actions are first encoded in the dorsomedial striatum in rodents (corresponding to the caudate in primates), and when the actions become habitual, encoding of the behavior is transferred to the dorsolateral striatum (the putamen in primates) (Yin, 2004; Yin, 2005; Yin, 2006). Furthermore, limbic structures such as the amygdala and hippocampus also project to the striatum, allowing information about the emotional valence and episodic memory of external stimuli to influence the cortico-striatal-thalamo-cortical circuitry (McDonald, 1991; Jennings, 2013; Stuber, 2011). Taken together, the striatum functions as a node that integrates information about the motivational level, history of reinforcement learning, past memories and emotional content of stimuli to influence motor behavior. Defects in the striatum could therefore profoundly affect the proper functioning of the cortico-striatal-thalamo-cortical circuitry, potentially leading to the aberrant behaviors observed in OCD.

## *1.2 Mutant mouse models of OCD*

The significant genetic contribution to the etiology of OCD has led to the generation of mutant mouse models to elucidate of the pathophysiology underlying OCD (Ting, 2011). Genetic mouse models enable the use of genetic, biochemical and electrophysiological techniques to dissect the molecular pathways, cell types and brain circuitry defects that result in OCD. Three mouse models of OCD and OC-spectrum disorders have been reported recently: the *Sapap3*-null (*Sapap3*$^{-/-}$), *Slitrk5*-null (*Slitrk5*$^{-/-}$) and *Hoxb8*-null (*Hoxb8*$^{-/-}$) mouse models (Welch, 2007; Shmelkov, 2010; Chen, 2010).

Three key criteria are used to determine the effectiveness of an animal model to model an illness: face, construct and predictive validities. Face validity refers to the ability of the animal model to recapitulate the phenotype of the disease. For instance, compulsive grooming is interpreted as ethnologically equivalent to compulsive cleaning in patients with OCD. Construct validity means the model shares the same biological etiology with patients, such as having similar genes mutated or similar brain circuit defects, such as the cortico-striatal-thalamo-cortical circuitry defect observed in OCD. Predictive validity points to the ability of the model to respond to proven treatments in patients, for example selective serotonin reuptake inhibitors (SSRIs) in OCD. Of the various mice models for OCD reported so far, only the *Slitrk5*$^{-/-}$ and *Sapap3*$^{-/-}$ mouse models have met face, construct and predictive validities for modeling OCD. These mutant mice lack genes that play different roles in the cortico-striatal-thalamo-cortical

circuit, but they are required for homeostatic plasticity, the global and proportional scaling of synapses in neural networks that ensures the stability and proper functioning of neural circuits (Stellwagen, 2006; Pascual, 2012).

**Table 2: Summary of knockout mouse models of OCD**

| Gene | Role and expression of gene | Behavioral phenotypes | Treatment |
|---|---|---|---|
| *Hoxb8* | Transcription factor that enables differentiation and maintenance of microglia | Repetitive grooming on body | Transplantation of wildtype bone marrow into irradiated mice |
| | | Allogrooming of cagemates | |
| | | Attenuated response to nociceptive and thermal stimuli | Acute subcutaneous lidocaine injection |
| | | Abnormal clasping reflex of limbs | |
| *Slitrk5* | Postsynaptic adhesion protein that promotes neurite outgrowth and excitatory synapse maturation in cortical neurons and MSNs | Repetitive grooming on head | Chronic intraperitoneal fluoxetine treatment |
| | | Increased anxiety-like behaviors | |
| *Sapap3* | Postsynaptic density scaffolding protein that orchestrates homeostatic scaling of excitatory synapses in cortical neurons and MSNs | Repetitive grooming on head | Chronic intraperitoneal fluoxetine treatment |
| | | Increased anxiety-like behaviors | |

### 1.2.1 Hoxb8-null mouse model

*Hoxb8* is a member of the Homeobox-containing complex (Hox) family of 36 transcription factors that regulate anterior-posterior anatomical patterning during embryonic development (Capecchi, 1997). Given the role of Hox proteins in morphogenesis, it is not surprising that *Hoxb8*$^{-/-}$ mice have numerous anatomical abnormalities such as a degenerated second spinal ganglion horn, a deformed first thoracic rib, and smaller dorsal horns at the lumbar spinal cord (Holstege, 2008; Chen S., 2010; Greer, 2002; van den Akker, 1999). As expected from the anatomical defects of the sensory inputs to the spinal cord, these mice exhibit attenuated responses to painful stimuli and impaired limb reflexes (van den Akker, 1999; Holstege, 2008).

Intriguingly, *Hoxb3*$^{-/-}$ mice also display self-inflicted skin lesions from repetitive grooming and increased allogrooming of cagemates (Greer, 2002). The abnormal grooming behavior is attenuated by acute subcutaneous lidocaine administration, suggesting a defect originating from sensory nerve terminals in the skin (Holstege, 2008). Interestingly, *Hoxb8* is not found in neurons in the central nervous system, but in microglia: It is required for the differentiation and maintenance of myeloid progenitor cells, one of two lineages that generate microglia (Chen S., 2010). In fact, transplantation of wild-type bone marrow into irradiated *Hoxb8*$^{-/-}$ mice alleviates repetitive grooming (Chen, 2010). Since microglia play an important role in the formation and pruning of dendritic spines (Clarke, 2013), the compulsive grooming behavior observed in *Hoxb8*$^{-/-}$

mice may result from aberrant homeostatic compensation for diminished sensory input. Although the *Hoxb8*$^{-/-}$ mouse model meets face validity for OCD, it currently lacks construct and predictive validity for modeling the disease. In contrast, the *Slitrk5*$^{-/-}$ and *Sapap3*$^{-/-}$ mouse models meet the three key criteria of face, construct and predictive validities.

### 1.2.2 Slitrk5-null mouse model

Slitrk5 is one of a family of six Slit- and Trk-like (Slitrk) proteins, post-synaptic adhesion molecules containing extracellular leucine-rich repeat (LRR) domains that regulate neurite outgrowth and synapse development, and it is primarily expressed at excitatory synapses in the cortex and striatum (Proenca, 2011; Shmelkov, 2010; Yim, 2013). While Slitrk 1, 2, 4 and 5 promote the maturation of excitatory synapses when bound to presynaptic protein tyrosine phosphatase-σ (PTPσ), Slitrk3 stimulates the formation of inhibitory synapses when bound to presynaptic PTPδ, indicating a role for Slitrks in regulating the excitatory-inhibitory balance of neurons (Yim, 2013; Takahashi, 2012). Genetic analyses have linked SLITRK1 to Gilles de la Tourette syndrome and trichotillomania, which like OCD share the common feature of distressing repetitive movements (Abelson, 2005; Zuchner, 2006). A GWAS has also identified PTPRD, the gene that codes for a presynaptic binding partner of Slitrk proteins, as an OCD candidate gene (Mattheisen, 2014).

*Slitrk1*$^{-/-}$ mice exhibit no compulsive behaviors, but instead show increased anxiety and depression-like behaviors that respond to clonidine, a treatment for Tourette syndrome (Katayama, 2010). In contrast, *Slitrk5*$^{-/-}$ mice are strikingly similar to *Sapap3*$^{-/-}$ mice, a mouse model for OCD. Like *Sapap3*$^{-/-}$ mice, *Slitrk5*$^{-/-}$ mice display compulsive grooming, leading to hemorrhaging skin lesions, and anxiety-like behavior (Shmelkov, 2010; Welch, 2007). Moreover, *Slitrk5*$^{-/-}$ mice exhibit increased activation of neurons in the orbitofrontal cortex and striatum, as indicated by expression of the immediate-early gene ΔFosB. Additionally, OCD-like behavior is alleviated by chronic fluoxetine treatment in these two mouse models (Shmelkov, 2010; Welch, 2007; Burguiere, 2013). As expected from the crucial role Slitrk5 plays in the growth of neural processes, *Slitrk5*$^{-/-}$ mice display reduced dendritic arborization of MSNs, decreased surface expression of ionotropic glutamate receptors, and a smaller AMPAR-mediated cortico-striatal population spike (Shmelkov, 2010).

### 1.2.3 Sapap3-null mouse model

Mice lacking SAP90/PSD95-associated protein 3 (SAPAP3, also known as DLGAP3) display compulsive grooming resulting in bloody skin lesions (especially on the head), and heightened anxiety-like behavior in the light-dark box, elevated zero maze and open field test (Welch, 2007). Both compulsive grooming and anxiety-like behavior in *Sapap3*-mutant mice are alleviated by fluoxetine, a serotonin-selective

reuptake inhibitor that is a first-line pharmaceutical treatment for OCD. Mirroring human patients with OCD, *Sapap3*$^{-/-}$ mice exhibit dysfunctional cortico-striatal transmission: The cortico-striatal population spikes recorded from knockout animals *Sapap3*$^{-/-}$ mice have a reduced AMPAR component, and an increased *N*-methyl-D-aspartate receptor (NMDAR) component.

SAPAP3 belongs to a family of four scaffolding proteins that orchestrates activity-dependent homeostatic scaling of excitatory synapses (Shin, 2012; Zheng, 2011). Of the four SAPAP isoforms, only SAPAP3 is expressed at the post-synaptic density of cortico-striatal excitatory synapses in the striatum (Welch, 2007). Therefore, in the striatum loss-of-function mutations in *Sapap3* are unlikely to be compensated through the upregulation of the other three isoforms at the cortico-striatal synapse.

As mentioned earlier, rare missense mutations and single nucleotide polymorphisms in *Sapap3* have been found to be correlated with OCD and trichotillomania by exon sequencing of the genomes of patients (Zuchner, 2009; Boardman, 2011; Bienvenu, 2009). Furthermore, the human *Sapap3* gene is located on chromosome 1, which is shown to be linked to OCD in the OCD Collaborative Genetics Study (OCGS) (Samuels, 2006). Moreover, two separate GWAS have implicated DLGAP1 (also known as *Sapap1*), a *Sapap* isoform, in OCD (Mattheisen, 2014; Steward, 2013).

Like OCD patients, hyperactivity of medium spiny neurons is observed in *Sapap3*$^{-/-}$ mice basally and during grooming using *in vivo* single-cell recordings, and activation of fast-spiking parvalbumin inhibitory interneurons in the striatum rescues compulsive grooming in these mice (Burguiere, 2013). Furthermore, chronic (but not short-term) activation of the medial orbitofrontal cortex to medial striatum pathway can induce repetitive grooming in wildtype mice (Ahmari, 2013). These studies suggest that hyperactivity of the cortico-striatal circuit is a consistent feature in both OCD patients and mouse models of the disorder.

## *1.3 Role of ΔFosB in neuropsychiatric disorders*

Unlike the other Fos isoforms, such as c-Fos, Fra1 and Fra2, which are expressed acutely and transiently during neuronal activity and develop tolerance (reduced expression) with repeated neuronal activity, ΔFosB levels gradually accumulate with sustained, chronic neuronal activation (Nestler, 2001). ΔFosB, a spliceoform of FosB that lacks two PEST (P, proline; E, glutamic acid; S, serine; and T, threonine-rich) protein degradation sequences at its carboxy-terminal, persists for weeks to months in the brain after the initial environmental stimuli (e.g., cocaine consumption, electroconvulsive therapy, or chronic stress) that triggered the initial neuronal activity (Nakabeppu, 1991; Nestler, 1999; Hiroi, 1998; Perrotti, 2004). With its long half-life, ΔFosB dimerizes with c-Jun to form a long-acting version of activator protein 1 (AP-1), a transcription factor that regulates numerous genes (Nestler, 2008; Vialou, 2010; Nestler, 2001). In addition, ΔFosB can also regulate genes through the epigenetic modification of chromatin, such as histone acetylation and methylation (Nestler, 2008). Rodent studies have shown that aberrant expression of ΔFosB mediates numerous pathological behaviors resulting from striatal dysfunction, such as drug addiction, social avoidance, learned helplessness, L-DOPA-induced dyskinesia, tardive dyskinesia, and compulsive behaviors.

### 1.3.1 ΔFosB in the nucleus accumbens

The role of ΔFosB, a splice variant of FosB formed during chronic activity, in the nucleus accumbens has been extensively studied. Exposure to drugs of abuse like cocaine increase ΔFosB levels in D1 MSNs of the nucleus accumbens, and overexpression of ΔFosB in the nucleus accumbens in naïve animals results in increased motivation to seek out artificial and natural rewards, such as cocaine, sex, running and sucrose (Kelz, 1999; Wallace, 2008; Werme, 2002). Therefore, increased ΔFosB in the nucleus accumbens is believed to mediate compulsive drug-seeking behavior in cocaine and methamphetamine addiction, and might play a role in other types of addiction. On the other hand, an inadequate increase in ΔFosB in the nucleus accumbens after chronic stress is associated with decreased resilience in major depressive disorder (Vialou, 2010). Mice with lower levels of ΔFosB after social isolation or social defeat display a greater despair-like phenotype in social avoidance and forced swim tests after chronic social defeat paradigms, while overexpression of ΔFosB in the nucleus accumbens alleviates depression-like behavior (Vialou, 2010). Correspondingly, patients suffering from major depressive disorder have lower levels of ΔFosB in the nucleus accumbens (Vialou, 2010). Therefore, ΔFosB in the nucleus accumbens is proposed to set the level of motivation in goal-directed behaviors.

**Table 3: Abnormal behaviors associated with ΔFosB expression**

| Brain region | ΔFosB expression | Rodent phenotype | Associated clinical disorder |
|---|---|---|---|
| Nucleus accumbens | Increased in D1 MSNs by cocaine exposure | Increased rewarding responses to cocaine in Conditioned Place Preference, Self-Administration and Progressive Ratio Assays | Cocaine addiction |
| | Insufficient increase after social isolation or social defeat | Increased social avoidance and increased immobility in Forced Swim Test | Major depressive disorder |
| Dorsolateral striatum (Putamen) | Increased in D1 MSNs by L-DOPA administration | Increased abnormal involuntary movements | L-DOPA-induced dyskinesia |
| | Increased in D2 MSNs by haloperidol | Increased rigid immobility (catalepsy) | Tardive dyskinesia and dystonia |
| Dorsomedial striatum (Caudate) | Increased in D1 MSNs in *Sapap3*$^{-/-}$ mice | Increased repetitive grooming on face | Obsessive-compulsive disorder |

### 1.3.2 ΔFosB in the dorsolateral striatum

While ΔFosB in nucleus accumbens plays a key role in increasing motivation, ΔFosB in the putamen (which corresponds to the dorsolateral striatum in rodents) affects motor activity. Evidence from rodent studies indicate that accumulation of ΔFosB in the dorsolateral striatum disrupts motor control. Elevation of ΔFosB in direct-pathway medium spiny neurons (D1 MSNs) mediates the abnormal uncontrollable movements of L-DOPA-induced dyskinesia (LID), while increases of ΔFosB in indirect-pathway medium spiny neurons underlie the extra-pyramidal side-effects of haloperidol, such as tardive dyskinesia, dystonia and parkinsonism (Bonito-Oliva, 2011).

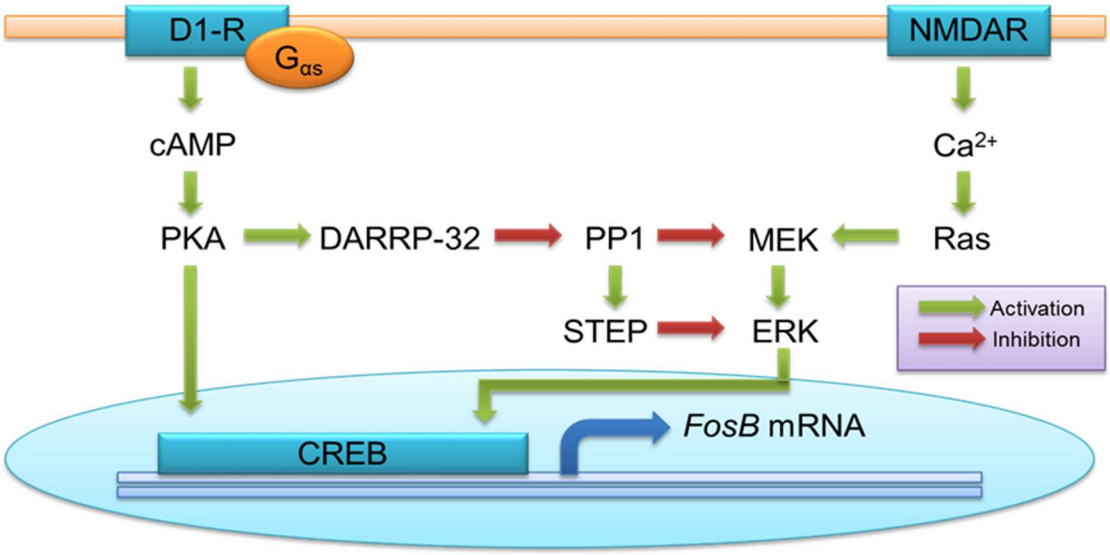


**Figure 3: Intracellular signaling pathways that promote *FosB* transcription**

ΔFosB is implicated in the pathogenesis of L-DOPA-induced dyskinesia (LID). Knock-down of FosB or overexpression of ΔJunD, a dominant-negative of ΔFosB, decreases L-DOPA-induced involuntary movements (Anderson, 1999; Berton, 2009), whereas overexpression of ΔFosB exacerbates LID (Cao, 2010). In LID, L-DOPA-mediated activation of sensitized dopamine 1a receptors (D1R) results in the activation of the cAMP/PKA/DARPP-32/PP-1 pathway, which in turn promotes ERK signaling, Both PKA and ERK phosphorylate CREB to activate its transcriptional activity, which leads to the transcription of ΔFosB mRNA. Conversely, in haloperidol-induced extrapyrimidal symptoms, blockade of dopamine 2 receptors (D2R) results in disinhibition of A2A receptor signaling, which also activates the cAMP/PKA pathway, but in indirect-pathway medium spiny neurons. Since direct-pathway medium spiny neurons promote movement, whereas indirect-pathway medium spiny neurons inhibit movement, the accumulation of ΔFosB in these two pathways mediate opposite effects.

### 1.3.3 ΔFosB in the dorsomedial striatum

Since the dorsomedial striatum of rodents (which corresponds to the caudate in primates) is involved in the learning of action-outcome associations and reinforcement learning (Brigman, 2013; Thorn, 2010), it can be inferred that increased ΔFosB would result in aberrant behaviors such as habit formation or even compulsive behaviors. Indeed, increased ΔFosB levels have been observed in the striatum of *Sapap3*$^{-/-}$ and *Slitrk5*$^{-/-}$ mice, two mouse models of OCD. In *Sapap3*$^{-/-}$ mice, FosB is significantly elevated in MSNs, especially D1 MSNs, and more D1 MSNs are also activated during grooming. In addition, cell-type specific knock-down of FosB in D1 MSNs (but not D2 MSNs) rescued compulsive grooming. Dysregulated gene expression resulting from the overexpression of FosB results in an increase in GluN2B expression at the post-synaptic density of *Sapap3*-null mice, and antagonism of GluN2B-containing NMDAR reduces OCD-like behavior. Upregulation of GluN2B expression in turn results in more silent synapses, immature synapses that express GluN2B-containing NMDARs but no AMPARs, and aberrant silent synapse formation mediates the cortico-striatal transmission defect observed in mouse models of OCD (Wan Y., 2011).

External stimuli that increase ΔFosB in rodents may possibly have links to compulsive behavior. Cocaine consumption increases ΔFosB levels primary in D1 MSNs in rodents; cocaine consumption is a risk factor for OCD in patients (Nestler, 2001; Crum, 1993). Moreover, stress (such as chronic restraint stress and social defeat stress)

increases ΔFosB levels in MSNs in rodents; stress is known to exacerbate obsessions and compulsions in patients with OCD (Perrotti, 2004; Vialou, 2010; American Psychiatric Association, 2000; Lochnet, 2001; Nacasch, 2011).

## *1.4 ΔFosB and synaptic plasticity*

ΔFosB dimerizes with c-Jun to form activator protein 1 (AP-1), a transcription factor with numerous gene targets, and also manipulates gene expression epigenetically through histone methylation and acetylation. For instance, ΔFosB upregulates GluA2, Cdk5, NFκB, GluN2B and SC1 transcription, while it downregulates c-fos and dynorphin (Kelz, 1999; Vialou, 2010). Since ΔFosB, a spliceoform of FosB that lacks protein degradation sequences at its carboxy-terminal, stays in the brain for weeks to months, it can mediate long-lasting and profound effects on gene expression (Nakabeppu, 1991).

**Table 4: Genes regulated by ΔFosB and their roles in synaptic plasticity**

| Gene product | Regulation | Role |
|---|---|---|
| GluA2 | Up | AMPAR subunit required for LTP and LTD |
| Cdk5 | Up | Kinase that regulates GluN2B subunit expression |
| NFκB | Up | Transcription factor that promotes synaptic plasticity |
| SC1 | Up | Extracellular matrix protein that promotes plasticity |
| GluN2B | Up | NMDAR subunit that promotes LTP through its slow channel kinetics |

### 1.4.1 Hebbian plasticity

Many gene targets of ΔFosB exert profound effects on Hebbian synaptic plasticity, namely long-term potentiation (LTP) and long term depression (LTD). In general, many genes upregulated by ΔFosB promote Hebbian plasticity, while many

genes downregulated by ΔFosB prevent Hebbian plasticity. For instance, c-fos and dynorphin, which are downregulated by ΔFosB, prevent neuronal damage from excitotocity and counteract the synaptic changes in addiction, respectively (Butelman, 2012; Zhang, 2002). In contrast, GluA2 is upregulated. It is an AMPAR subunit that is required for long-term depression (LTD) and can assist long-term potentiation (LTP), the two main mechanisms for Hebbian plasticity (Toyoda, 2007; Granger, 2013; Passafaro, 2003). Furthermore, other genes upregulated by ΔFosB, NFκB, a transcription factor, and SC1, an extracellular matrix protein, have both been shown to promote synaptic plasticity (O'Neill, 1997; Lively, 2008). Likewise, Cdk5, a kinase that regulates surface expression and degradation of the more calcium-permeable GluN2B subunit of the NMDA receptor, is also upregulated (Lai, 2009; Jessberger, 2009; Plattner, 2014). Moreover, GluN2B itself is upregulated by ΔFosB (Qiang, 2005; Grueter, 2013).

GluN2B, an NMDAR modulatory subunit, is highly expressed in the cortex and striatum (Monyer, 1994). At functional synapses, GluN2B expression endows NMDARs with slow channel kinetics and binds to calcium/calmodulin-dependant kinase II (CaMKII) at its intracellular carboxy-terminal (Zhou, 2007; Foster, 2010; Kerchner, 2008). This promotes long-term potentiation (LTP) since the slow channel kinetics prolongs the calcium influx into the cell. Conversely, at immature, silent synapses, GluN2B signaling prevents the recruitment of AMPARs to AMPAR-silent synapses (Hall, 2007).

### 1.4.2 Silent synapses

Silent synapses, immature synapses which contain GluN2B-containing NMDARs but no detectable AMPARs, are the substrates for new functional excitatory synapses (Kerchner, 2008). During neural development, GluN2B is necessary and sufficient for the creation and conservation of silent synapses (Hall, 2007; Gray, 2011; Lee, 2010; Kerchner, 2008; Hanse, 2013). Co-ordinated pre and postsynaptic neuronal activity results in the unsilencing and maturation of synapses, which is marked by a GluN2B-to-GluN2A switch in NMDAR composition.

Whereas silent synapses on glutaminergic neurons are largely absent in the mature nervous system after a critical period of heightened neuronal plasticity during development (Ashby, 2011), silent synapses on GABAergic neurons such as MSNs persist into adulthood (Huang, 2009; Brown, 2011; Grueter, 2013). Between 10 to 30% of MSNs have silent synapses, which are normally found on D2 MSNs at physiological conditions (Grueter, 2013). However, in certain pathological conditions such as cocaine addiction, silent synapses are increased primarily in D1 MSNs, probably because ΔFosB increases silent synapses in D1 MSNs (Huang, 2009; Grueter, 2013). Viral-mediated overexpression of ΔFosB in the striatum, which upregulates GluN2B expression, decreases the AMPAR/NMDAR ratio, increases the proportion of GluN2B-containing NMDARs, and increases the proportion of silent synapses at cortico-striatal connections in D1 MSNs, findings that are similar to the electrophysiological abnormalities reported

in *Sapap3*$^{-/-}$ mice (Wan Y., 2011; Grueter, 2013). Indeed, the preferential expression of silent synapss on D1 MSNs may contribute to the impaired cortico-striatal neurotransmission and imbalance in the direct and indirect pathways that characterize compulsive behaviors.

### 1.4.3 Homeostatic scaling

Since Hebbian plasticity is inherently destabilizing, neurons employ homeostatic plasticity to maintain the stability of neuronal networks (Davis, 2013). In particular, homeostatic scaling – the global and proportional scaling of synaptic weights – is essential for the normal functioning of neural networks (Turrigiano, 2004; Burrone, 2003; Davis, 2013). Under normal conditions, microglia secrete basal levels of tumor necrosis factor alpha (TNF-$\alpha$) and adenosine triphosphate (ATP) to stimulate astroglia expressing TNF receptor 1 (TNFR1) (Stellwagen, 2006). The activated astroglia modulate excitatory synapse strength by releasing glutamate that activates perisynaptic metobotropic glutamate receptors (mGluRs) (Pascual, 2012). In addition, during periods of heighted synaptic activity and calcium influx, calcium/calmodulin-dependent protein kinase II-$\alpha$ (CaMKII$\alpha$) phosphorylates SAPAPs at the PSD95-binding domain to trigger the scaling down of active synapses (Shin, 2012). Conversely, during periods of low activity, CaMKII$\beta$ phosphorylates SAPAPs at the myosin-binding domain to recruit ionotrophic glutamate receptors to scale up weak synapses.

Mouse models of OCD lack genes that are implicated in homeostatic scaling. For instance, OCD-like behavior has been observed in mutant mice with deletions in *Hoxb8*, which is required for microglia maintenance and differentiation (Chen, 2010), *Sapap3*, which orchestrates homeostatic scaling (Shin, 2012), and *Slitrk5*, which promotes excitatory synapse maturation (Shmelkov, 2010). Homeostatic scaling is especially important in the developing brain, where newly created neurons must function properly as new synapses are being formed, potentiated and eliminated. Corresponding to the observation that the developing brain is more vulnerable to insults that cause OCD in adulthood, childhood trauma is a risk factor for developing OCD in adulthood (Lochnet, 2001). Nonetheless, though homeostatic plasticity has been extensively studied *in vitro* and is starting to be examined *in vivo* in rodents, its role in human disease is relatively obscure (Turrigiano, 2004; Keck, 2013).

# Chapter 2: Methods

## 2.1 Animals

*Sapap3*$^{-/-}$ mice were generated by homologous recombination in R1 embryonic stem cells. D1GFP (X60), D2GFP (S118), D1-Cre (EY217) and A2A-Cre (KG139) mice were obtained from GENSAT. D1-TdTomato mice were gifts from Nicole Calakos, Duke University (Shuen, 2008); *Slitrk5*$^{-/-}$ mice were gifts from Francis Lee, Weill-Cornell Medical College (Shmelkov, 2010). Unless otherwise stated, 3 to 4 month old C57BL/6 mice of both sexes were used. All assays and analyses were performed without knowledge of the animals' genotype. Protocols involving mice were approved by the Institutional Animal Care and Use Committees of the Massachusetts Institute of Technology and Duke University.

## 2.2 Nuclear extraction

Microdissected striata from mice were processed for nuclear extraction using standard protocols. Briefly, brain tissue was homogenized in ice-cold Lysis Buffer (1 M HEPES pH 7.9, 3 M KCl, 1 M $MgCl_2$, 10% NP40, 1 M DTT, Roche Complete Mini protease inhibitor tablets) and centrifuged at low speed (1500*g* for 5 minutes at 4 $^{o}$C). The nuclear pellet was washed by suspension and low-speed centrifugation in ice-cold Low Salt Solution (1 M HEPES pH 7.9, 80% glycerol, 1 M $MgCl_2$, 3 M KCl, 0.5 M EDTA, 1

M DTT, protease inhibitors). The nuclear proteins were dissolved by incubation for 1 hour on ice with vigorous vortexes every 15 minutes in High Salt Solution (1 M HEPES pH 7.9, 80% glycerol, 1 M $MgCl_2$, 3 M KCl, 0.5 M EDTA, 1 M DTT, protease inhibitors), followed by ultracentrifugation at 109,000*g* for 1 hour. After ultracentrifugation, the supernatant (nuclear protein extract) was collected.

## *2.3 Post-synaptic density (PSD) extraction*

PSD extraction was conducted using standard protocols. Briefly, microdissected striata from mice were homogenized in 1 ml ice-cold HEPES-A Solution (4 mM HEPES pH 7.4, 0.32 M sucrose in Roche Complete protease inhibitors), and the homogenate was centrifuged at 900*g* for 15 minutes at 4°C. The supernatant (whole brain lysate) was collected and centrifuged at 18,000*g* for 15 minutes to isolate the pellet (crude synaptosomal fraction). The crude synaptosomal fraction was suspended in 1 ml ice-cold HEPES-A Solution and centrifuged again at 18,000*g* for 15 minutes to wash the pellet. The washed pellet was suspended in 1 ml ice-cold HEPES-B Solution (4 mM HEPES pH 7.4, with protease inhibitors), slowly rotated at 4 °C for 1 hour, and spun down in an ultracentrifuge at 25,000*g* for 20 minutes at 4 °C to yield a supernatant (crude synaptic vesicle fraction) and pellet (lysed synaptosomal membrane fraction). The lysed synaptosomal membrane fraction was resuspended in 380 μl of ice-cold HEPES-C Solution (50 mM HEPES pH 7.4, 2 mM EDTA and protease inhibitors) and 20 μl of 10%

Triton-X in HEPES-C Solution, rotated at 4 °C for 15 minutes, and centrifuged at 32,000*g* for 20 minutes in an ultracentrifuge. The resultant pellet (PSD-1T fraction) was suspended in 475 μl of HEPES-C Solution and 25 μl of 10% Triton-X in HEPES-C Solution, rotated at 4 °C for 15 minutes, followed by ultracentrifugation at 200,000*g* for 20 minutes. The extracted pellet (PSD-2T fraction) was suspended in 90 μl of HEPES-C Solution, 13.05 μl of 20% SDS and 40.5 μl of 9 M Urea.

## 2.4 Western blotting

Western blots were performed under standard conditions, with 100 μg of nuclear protein or 2 μg of PSD protein loaded in each well of 10% SDS-PAGE gels. Protein concentration was measured using a Pierce BCA Protein Assay Kit (Thermo Scientific). Primary antibodies used were rabbit anti-ΔFosB polyclonal antibodies (1:250, Santa Cruz Biotechnology, sc-48), rabbit anti-Lamin A/C polyclonal antibody (1:250, Santa Cruz Biotechnology, sc-20681), rabbit anti-GluA1 polyclonal antibody (1:250, Abcam, AB37332), mouse anti-GluA2 monoclonal antibody (1:250, Neuromab, L21/32), mouse anti-GluN2B monoclonal antibody (1:250, Neuromab, N59/36), mouse anti-GluN2A monoclonal antibody (1:250, Millipore, MAB2516), mouse anti-GluN1 monolconal antibody (1:250, BD Biosciences, 556308), and mouse anti-α-tubulin monoclonal antibody (1:10,000, Sigma, T5168) diluted in 5% Milk-TBS. Protein bands were visualized in the Odyssey CLx Infrared Imaging System (Li-Cor) using IRDye 680RD

goat anti-mouse and 800CW goat anti-rabbit secondary antibodies (1:5,000, Li-Cor). Protein blot band intensities were quantified using ImageJ software (NIH), and normalized to either Lamin A or $\alpha$-tubulin signals.

## 2.5 Immunohistochemistry

Mouse brains were perfused, sectioned, blocked, labeled and imaged using standard protocols. For ΔFosB analyses, mice were obtained directly from their home cages for perfusion. After isoflourane administration, mice were transcardially perfused with PBS followed by 4% paraformaldehyde dissolved in PBS, and the perfused brains were incubated in 4% paraformaldehyde overnight. 50 μm coronal vibrotome sections were blocked in Blocking Solution (5% normal goat serum, 2% BSA, 0.2% triton X-100 in PBS, or 0.1 M Tris, pH 7.6 for anti-ChAT antibodies) for 1 hour at room temperature. The primary antibodies used were: rabbit anti-ΔFosB polyclonal antibody (1:250, Santa Cruz Biotechnology sc-48), rabbit anti-c-Fos polyclonal antibody (1:1000, Chemicon, PC-38), mouse anti-parvalbumin monoclonal antibody (1:5,000, Swant, PV-28), goat anti-choline acetyltransferase polyclonal antibody (1:250, Millipore, AB144P), rabbit anti-substance P polyclonal antibody (1:1000, Abcam, ab10353), and rabbit anti-met-enkephalin polyclonal antibody (1:1000, Chemicon, AB5026). Slices were incubated overnight at 4 $^{o}$C in primary antibodies, washed three times in PBS, and incubated for three hours at room temperature with goat Alexa488 and Alexa555-conjugated anti-

mouse, anti-rabbit or anti-goat secondary antibodies (1:1,000, Jackson Immunoresearch). Next, the sections were washed three times in PBS, and mounted in Vectashield Mounting Medium (Vector Labs). The Olympus Fluoview FV1000 confocal microscope, Olympus BX61 epifluorescence microscope and Olympus CellSans Dimension software were used to image the sections and quantify fluorescence intensities. For c-Fos analyses, quantification of c-Fos$^+$ puncta was conducted using Metamorph software (Molecular Devices).

## *2.6 Primary cortico-striatal cultures*

The striatum and cortex of post-natal day 0 (P0) pups were microdissected in ice-cold Hibernate-A calcium-free medium (Brain Bits). The brain tissue was dissociated for 25 minutes using 400 μg/ml papain in 5 ml Hiberate-A calcium-free media, followed by 5 minutes of DNA digestion by adding 20 μl of 10 mg/ml DNAaseI, both at 37 $^{o}$C. After washing the dissociated brain tissue with 5 ml Hibernate-A calcium-free medium, the tissue was dissociated into single cells by pipetting slowly and gently through a fire-polished glass Pasteur pipette in Hibernate-A Complete Medium (2% B-27 serum-free supplement (Gibco) and 0.5 mM GlutaMAX supplement (Gibco) in Hibernate-A calcium-free medium), and then filtered through a 40 μM cell strainer. The density of the dissociated neurons were counted using a hemocytometer, and resuspended in Plating Medium (10% heat-inactivated fetal bovine serum (Hyclone), 2% B-27

supplement, 2 mM GlutaMAX supplement in Neurobasal-A medium (Gibco)). The resuspended neurons were added to a 24-well plate holding poly-D-lysine and laminin-coated glass coverslips at a density of 0.1-0.2 million neurons per well, with 80% striatal neurons and 20% cortical neurons. Plating medium was replaced by Neurobasal-A Complete Medium (2% B-27 serum-free Supplement, 0.5mM GlutaMAX supplement in Neurobasal-A medium) 4 hours after plating. Half of the medium (500 μl per well) was replaced with freshly prepared Neurobasal-A Complete Medium at 5 days in vitro (DIV).

## *2.7 Immunocytochemistry*

At 10 DIV, the cortico-striatal cultures were incubated either with 40 μM bicuculline, 2 μM tetrodotoxin or vehicle (Neurobasal-A Complete Media) for 48 hours. Next, each coverslip was washed once with 1 ml PBS, and then fixed in 1 ml of 4% paraformaldehyde (dissolved in PBS) for 15 minutes. The neurons were then incubated in 1 ml of Blocking Solution (5% normal goat serum, 2% BSA, 0.2% triton X-100 in PBS) for 1 hour. Primary antibodies used were: anti-DARPP32 mouse monoclonal antibody (1:1000, BD Biosciences, 611520) and anti-ΔFosB rabbit polyclonal antibody (1:250, Santa Cruz Biotechnology, sc-48). Each coverslip was incubated overnight at 4 $^{o}$C in 100 μl of primary antibody diluted in Blocking Solution. After three washes with PBS, the coverslips were incubated in goat anti-mouse Alexa488-conjugated and anti-rabbit

Alexa555-conjugated secondary antibodies (1:1000, Jackson Immunoresearch) for 1 hour at room temperature. The coverslips were washed three times in PBS and then mounted in Vectashield Mounting Medium (Vector Labs). The Olympus Fluoview FV1000 confocal microscope and Olympus CellSans Dimension software were used for imaging and fluorescence quantification.

## *2.8 Real-time quantitative PCR*

The striatum of adult mice were microdissected on ice, and RNA was isolated using Trizol reagent (Invitrogen). Briefly, brain tissue was homogenized in 1 ml of ice-cold Trizol reagent, and incubated for 5 minutes at room temperature to allow dissociation of nucleoprotein complexes. 0.2 ml of chloroform was added, followed by room-temperature incubation for 2 minutes. The samples were then centrifuged at 12,000*g* for 15 minutes, and the colorless upper aqueous phase was retrieved. RNA was precipitated by mixing the aqueous phase with 0.5 ml of isopropanol, followed by room-temperature incubation for 10 minutes and centrifugation at 12000*g* for 10 minutes. The RNA pellet was washed once by centrifugation in 1 ml of 75% ethanol at 7500*g* for 5 minutes, air-dried, and dissolved in 20 μl of RNAase-free water at 55$^{o}$C. The RNA was reverse transcribed using the iScript cDNA Synthesis Kit (Bio-Rad) with 2 μg of RNA in a 20 μl reaction, according to manufacturer's instructions (5 minutes at 25 $^{o}$C, 30 minutes at 42 $^{o}$C, and 5 minutes at 85 $^{o}$C in a thermocycler). The complementary DNA (cDNA)

was amplified in a 20 μl reaction (0.03 μl of the cDNA, 125 nM of each primer and Bio-Rad iQ SYBR Green Supermix) using a CFX384 Real-Time PCR System with the following conditions: 3 minutes at 95 °C, 35 cycles of denaturation at 95 °C for 15 minutes and annealing/extension at 57 °C for 30s, followed by 55-95 °C at 0.5 °C increments, 2 s per step. Samples were run in triplicates and repeated twice. Messenger RNA quantification was computed using the $\Delta\Delta C_t$ method with GAPDH used as the internal normalization control. The primer sequences were obtained from the GETPrime Database (Gubelmann, 2011), except for the primers for GAPDH and ΔFosB:

GAPDH-F 5′-AGG,TCG,GTG,TGA,ACG,GAT,TTG-3′

GAPDH-R 5′-TGT,AGA,CCA,TGT,AGT,TGA,GGT,CA-3′

ΔFosB-F 5′-AGG,CAG,AGC,TGG,AGT,CGG,AGA-3

ΔFosB-R 5′-GCC,GAG,TTG,AAC,TTC,ACT,CGG-3′

Cdk5-F 5′- GAT,TGT,GAA,GTC,ATT,CCT,CTT,CC-3′

Cdk5-R 5′-TTC,AGG,TCC,CTA,TGT,AGC,AC-3′

Sparcl1-F 5′-GAA,AGC,TGA,GAG,CTC,ACC,A-3′

Sparcl1-R 5′-GAA,GTT,CGT,GCA,AGA,ACC,AG-3′

Nfkb-F 5′-AGC,ACA,TAG,ATG,AAC,TCC,G-3′

Nfkb-R 5′-CTG,TAA,AGC,TGA,GTT,TGC,G-3′

Pdyn-F 5′-GTA,AGC,AGG,TCA,TTC,ATC,CC-3′

Pdyn-R 5′- ACA,CAT,AAC,TCA,CCC,TGC,T-3′

Gria1-F 5′-CCC,AAC,AAT,ATC,CAG,ATA,GGG-3′

Gria1-R 5′-GTT,GTG,ACA,AAG,CAA,ACC,T-3′

Gria2-F 5′-GAG,TAG,ATC,GAG,CAG,AGG,A-3′

Gria2-R 5′-ACC,GCA,TTT,CTT,AAT,GAG,GA-3′

Grin1-F 5′-CAT,CTC,TAG,CCA,GGT,CTA,CG-3′

Grin1-R 5′-CAG,CTG,TGT,AGG,AGA,CAG,G-3′

Grin2a-F 5′-CAG,TGA,CAA,GAA,GTT,CCA,GAG-3′

Grin2a-R 5′-CTT,TCT,GTA,CTT,CCA,TTG,GGT-3′

Grin2b-F 5′-CTT,AAT,CTG,TCC,GCC,TAG,AG-3′

Grin2b-R 5′-ATC,TTC,AGC,TCG,TCG,ACT,C-3′

Grm1-F 5′-AGA,TTA,AGG,TCA,TAC,GGA,AAG,G-3′

Grm1-R 5′-CAT,CTT,GCA,CAA,ACT,CAT,TCT,C-3′

Grm5-F 5′-AAC,CCT,AAG,CTC,CAA,TGG,A-3′

Grm5-R 5′-TAT,GGA,CAG,ACA,GTC,GCT,G-3′

Grid1-F 5′-TCT,ATG,ACA,GCG,AGT,ATG,ATA,TCC-3′

Grid1-R 5′-GTA,AAG,AGA,CAT,CCA,GAC,CCA-3′

## *2.9 Virus production*

ΔFosB shRNA was designed using the 21 base-pair target sequence 5′-CTC,TTT,ACA,CAC,AGT,GAA,GTT -3′, and scrambled shRNA contained the 21 base-

pair sequence 5′-CGT,AAG,TGA,TGC,TTT,AAC,AGA-3′. The 21 base-pair sense and antisense sequences were connected by a hairpin loop, and followed by a poly(T) termination sequence. The ΔFosB shRNA and scrambled shRNA constructs were annealed from phosphorylated oligonucleotides, and cloned into dsAAV RSV GFP H1 933FF vectors (gift from Mark Kay, Stanford University) using BbsI restriction enzyme sites. DIO-ΔFosB-shRNA and ΔFosB-EGFP overexpression constructs were annealed from phosphorylated oligonucleotides and cloned into AAV constructs expressing EGFP (gifts from Karl Deisseroth, Stanford University). The TATA-loxP site containing an H1 promoter was modified from a TATA-lox site containing a U6 promoter. Adeno-associated viruses were produced by transfection of AAV293 cells (Stratagene) with three plasmids: an AAV ITR-containing vector plasmid (AAV-ΔFosB-shRNA , AAV-scrambled-shRNA or AAV-DIO-ΔFosB-shRNA ) along with RepCap (AAV2/8) and helper (pAd-ΔF) plasmids. 40 hours after transfection, the cells were lysed by a freeze-thaw procedure in a dry ice-ethanol bath. The cell lysate was incubated in benzoase nuclease (Sigma) to digest DNA contaminants, followed by ultracentrifugation at 80,000*g* to pellet the virus. The viral pellet was suspended in PBS and concentrated using Amicon Ultra-4 100 kDa filter units. Viruses were tested in HEK293 cells to determine expression before stereotaxic injection.

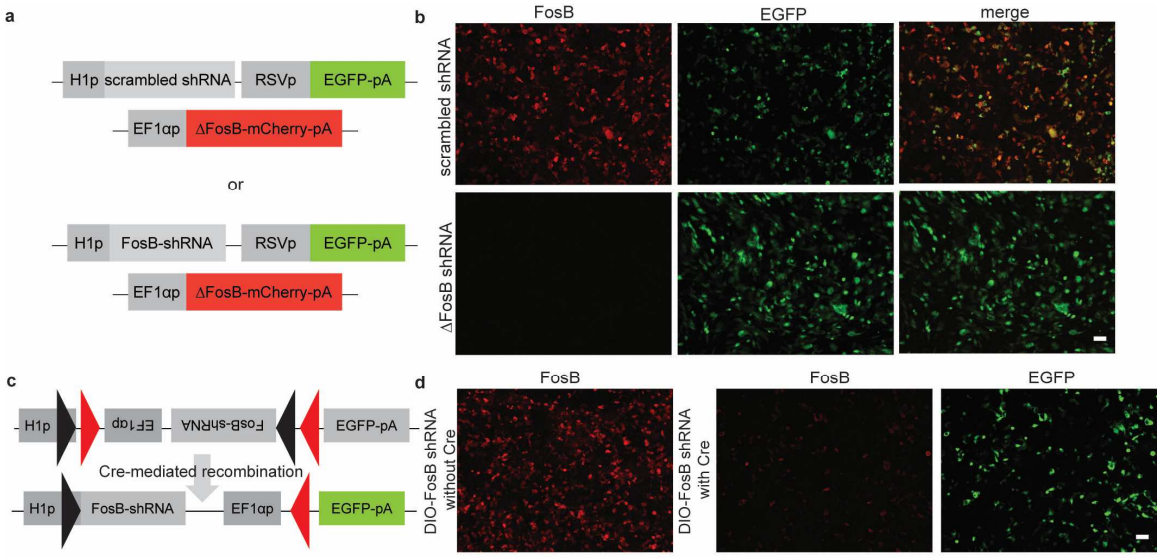


**Figure 4: Reduction in ΔFosB protein expression by ΔFosB shRNA. a, Diagrams of the ΔFosB-shRNA vector, which expresses both shRNA against ΔFosB and EGFP, control scrambled shRNA vector, and ΔFosB complementary DNA (cDNA) overexpression vector. b, Fluorescence images of HEK293 cells co-transfected with a ΔFosB overexpression vector (red) and an AAV vector expressing scrambled shRNA (green) showed no reduction in ΔFosB levels (red). In contrast, fluorescence images of HEK293 cells co-transfected with ΔFosB cDNA (red) and an AAV vector expressing ΔFosB shRNA (green) display a significant reduction in ΔFosB protein expression (red) after knock-down by the ΔFosB shRNA. c, Schematic of DIO-ΔFosB-shRNA vector, which expresses ΔFosB-shRNA and EGFP after Cre-mediated recombination. d, Fluorescence images demonstrating a reduction in ΔFosB levels (red) in HEK293 cells co-transfected with both Cre recombinase and the DIO-ΔFosB-shRNA vector (green). Scale bar: 10 μm. Graphs display means and s.e.m.**

## 2.10 Stereotaxic injection

Unless stated otherwise, 3 to 4 month old mice were anesthetized using 5% isofluorane and placed on a David Koph stereotaxic head frame for mice. 200 nl of concentrated AAV was infused using a WPI Micro4 microsyringe pump at a rate of 125 nl $min^{-1}$ into the caudate-putamen at each of the following 8 coordinates: anterior-posterior +0.98 mm; medial-lateral +1.8 and -1.8 mm; and dorsal-ventral 3.00, 3.17, 3.34, 3.51 mm. Infusion needles were left at the infusion site for 10 minutes before retrieval. Behavioral assays were conducted 2 to 4 weeks after viral infusion. For injection into postnatal day 21 (P21) mice, 180 nl of concentrated virus was infused at a rate of 125 nl $min^{-1}$ at the following coordinates: anterior-posterior +0.91 mm; medial-lateral +1.7 and -1.7 mm; and dorsal-ventral 2.80, 3.05, 3.30, 3.55 mm, and behavioral assays were conducted when the mice were 4 months old.

## 2.11 Behavioral assays

Quantification of grooming time, open field tests and elevated zero maze tests were conducted based on previously described protocols. To quantify grooming activity, animals were videotaped overnight, and the time spent grooming from 19:00 to 21:00 h was quantified by two independent observers using the Noldus Observer software. In the elevated zero maze, animals were placed in the closed arm of an elevated zero maze indirectly illuminated at 70 lux, and activity on the zero maze was videotaped over 5

minutes. The time spent in the open arms was scored from the videos as a measure of anxiety-like behavior. In the open field test, animals were positioned in an Omnitech Digiscan animal activity monitoring chamber (AccuScan Instuments), and the locations of the mice freely exploring the chamber were recorded automatically for 30 minutes by the bundled VersaMax software. The total distance moved was used to assess locomotor activity, and the distance travelled at the illuminated center of the chamber was used to determine anxiety-like behavior. Animals were habituated in the testing room for at least an hour before conducting the behavior assays.

## 2.12 Drug treatment

3 to 4 month-old *Sapap3*$^{-/-}$ and wildtype littermates were singly housed and randomly assigned to treatment and control groups. Behavioral assays and data analyses were conducted blinded to the animals' genotypes and to the identity of the drug and vehicle. The mice were randomized as follows: a mouse of genotype A was assigned to treatment X; another littermate, to treatment Y; a third littermate, to treatment X, until all the mice were separated into two treatment groups. The same procedure was done for genotype B. The vehicle used was 0.1 mg ml$^{-1}$ l-ascorbic acid (Sigma) dissolved in distilled water to prevent oxidative degradation of the drug. 20 mg kg$^{-1}$ of CP101,606 mesylate salt (Axon MedChem) dissolved in vehicle was administered *ad libitum* in the drinking water every day for two weeks. The drug and

vehicle were prepared every day to minimize photodegradation and blinded to the experimenter before drug administration. Video-recordings of grooming behavior were conducted before drug treatment, after one week of drug treatment, and two weeks after initiation of drug washout. Each video contains mice from all four groups, with a positive control (*Sapap3*$^{-/-}$ mouse treated with vehicle) and negative control (wildtype mouse treated with vehicle). Wildtype mice treated with vehicle were used as the standard for normal grooming behavior. Open field and zero maze tests were conducted after two weeks of drug treatment.

## 2.13 Electrophysiology

Acute coronal striatal slices were prepared from 2 to 3 month old mice. The mice were anesthetized with Avertin (50 mg kg$^{-1}$) and perfused through the heart with 20 ml of ice-old cutting solution containing (in mM): 30 NaCl, 4.5 KCl, 1.2 $NaH_2PO_4$, 194 sucrose, 26 $NaHCO_3$, 10 glucose, 0.2 $CaCl_2$, 8.0 $MgSO_4$ (pH 7.4, 295-305 mOsm), oxygenated with 95% $O_2$ and 5% $CO_2$. The slices were cut with a vibratome (Leica Microsystems) in cutting solution and recovered in artificial cerebrospinal fluid (ACSF) that contains (in mM): 119 NaCl, 2.3 KCl, 1.0 $NaH_2PO_4$, 26 $NaHCO_3$, 11 glucose, 1.3 $MgSO_4$, 2.5 $CaCl_2$ (pH 7.4, 295-305 mOsm) for 10 minutes at 32 $^{o}$C, followed by 1 hour at room temperature. Whole-cell patch-clamp recordings were acquired using a Multiclamp 700B amplifier (Molecular Devices) and Digidata 1440A, at 20 kHz and

filtered at 2 kHz. The slice was constantly perfused with oxygenated ACSF at 24 $^{o}$C at a rate of 1.5-2.0 ml $min^{-1}$. D1 and D2 MSNs were visualized by D1-TdTomato and D2GFP fluorescence. Pipettes were pulled in a horizontal pipette puller (P-87, Sutter Instruments) to a resistance of 3-4 MΩ and filled with internal solution containing (in mM): 110 CsOH, 110 d-gluconic acid, 15 KCl, 4 NaCl, 5 TEA-Cl, 20 HEPES, 0.2 EGTA, 5 lidocaine *N*-ethyl chloride, 4 ATP magnesium salt, and 0.3 GTP sodium salt (pH 7.3, 298-300 mOsm). Recordings were conducted in the presence of 100 μM picrotoxin to block $GABA_A$ receptors. Slices were incubated in either ACSF with 1mM glycine (vehicle) or 20 μM of CP101,606 mesylate salt (drug) dissolved in vehicle in a slice holding chamber starting 25 minutes prior to recording, and the drug or vehicle was continually perfused into the bath solution during recording. Miniature excitatory postsynaptic potentials (mEPSCs) were obtained in the presence of 1 μM TTX, and analyzed using Synaptosoft Mini Analysis Program blinded to genotype. Evoked excitatory postsynaptic currents (EPSCs) were evoked by a FHC local concentric bipolar stimulating electrode placed in the inner edge of the corpus callosum within the dorsal striatum. Paired-pulse ratio (PPR) was calculated as the ratio of the second peak current response to the first response, with an inter-stimulus interval of 50 ms and a holding potential of -70 mV. 15 PPRs, evoked every 30 seconds, were obtained from each cell.

## *2.14 Statistics*

Three independent experiments, using three or more biological replicates per group, were conducted, and sample sizes were based on previously published reports. Comparisons of two groups were performed using two-tailed *t* tests, and comparisons of three or more groups were conducted using analyses of variance (ANOVA) with post-hoc Bonferroni tests, unless stated otherwise. Assumptions of statistical tests were met, and significance was determined using $\alpha$=0.05. Statistics were analyzed on GraphPad Prism software. Graphs indicate mean±s.e.m. *P<0.05; **P<0.01; ***P<0.001.

# Chapter 3: Results

Homeostatic plasticity, compensatory adjustments in synaptic strengths to offset excessive excitation or inhibition, is crucial in the developing brain, where newly formed neurons must function normally while synaptic connections are being formed, strengthened and pruned (Turrigiano, 2004). Defective homeostatic plasticity during neuronal development has been postulated to cause several neuropsychiatric disorders, such as autism, schizophrenia and obsessive-compulsive disorder (OCD) (Ramocki, 2008; Davis, 2013; Pauls, 2014; Wondolowski, 2013). However, the molecular mechanisms linking impaired homeostatic plasticity to neuropsychiatric phenotypes are poorly understood. Here we report that compulsive grooming behavior in *Sapap3*-mutant mice (Welch, 2007), which lack a post-synaptic scaffolding protein that orchestrates homeostatic scaling (Shin, 2012), is caused by the elevation of ΔFosB, a highly stable transcription factor induced by chronic neuronal activity (Nestler, 2008). ΔFosB accumulation initiates during neurodevelopment, and occurs primarily in D1 dopamine receptor-expressing medium spiny neurons (D1 MSNs). Additionally, ΔFosB upregulates the expression of GluN2B, an *N*-methyl-D-aspartate glutamate receptor (NMDAR) subunit that generates silent synapses (Hanse, 2013; Gray, 2011; Hall, 2007; Huang, 2009; Brown, 2011). Furthermore, pharmacological antagonism of GluN2B restores excitatory synaptic transmission in D1 MSNs and rescues compulsive grooming. Therefore, we have introduced a molecular mechanism whereby aberrant

homeostatic plasticity causes pathological behavior, and in the process identified a novel drug target for compulsions. Indeed, this mechanism may be relevant for other neuropsychiatric disorders with neurodevelopmental etiologies.

## 3.1 Preface

Current evidence implicates cortico-striatal-thalamo-cortical circuit hyperactivity in the pathogenesis of obsessive compulsive disorder (OCD) (Pauls, 2014), a debilitating disorder that afflicts 1 to 3% of the world's population with recurring intrusive thoughts (obsessions) leading to irrational repetitive behaviors (compulsions) (Kessler, 2005). Imaging studies have consistently found increased activity in the orbital frontal cortex and the head of the caudate in patients with OCD (Menzies, 2008). In addition, deep brain stimulation (DBS) near the internal capsule, containing cortico-striatal axon bundles, ameliorates obsessions and compulsions in patients and its effects are reversed when DBS is stopped (Greenburg, 2006; Figee, 2013). Furthermore, in mice chronic (but not acute) stimulation of the cortico-striatal circuit is sufficient to induce persistent repetitive grooming behavior (Ahmari, 2013), and stimulation of striatal inhibitory interneurons alleviates compulsive grooming (Burguiere, 2013). Since this evidence is at odds with the observation of attenuated cortico-striatal excitatory synaptic transmission in OCD mouse models, such as *Sapap3*-null and *Slitrk5*-null mice (Welch, 2007; Shmelkov, 2010; Wan Y., 2011), we hypothesize that a maladaptive compensatory mechanism underlies OCD-like behavior.

While clinical manifestations and co-morbidities vary between patients with OCD, epidemiological and genetic studies indicate that OCD is heritable, with multiple alleles converging onto identical OCD symptoms (Nestadt, 2010). For instance, genetic

studies have linked loss-of-function *Sapap3* variants to OCD (Bienvenu, 2009; Zuchner, 2009; Boardman, 2011). Sapap3 belongs to a family of four scaffolding proteins that orchestrates the maturation and elimination of dendritic spines (Shin, 2012). In addition to *Sapap3*, OCD-like behavior has been reported in mice lacking other genes that also regulate spine dynamics, such as *Hoxb8* and *Slitrk5*. *Hoxb8* is required for the maintenance and differentiation of microglia, a key player in synapse stabilization and pruning (Chen, 2010; Clarke, 2013). Similarly, *Slitrk5* controls neurite outgrowth in cortical and striatal neurons (Shmelkov, 2010). Unrestrained growth and loss of dendritic spines may lead to chronic perturbations that result in the accumulation of ΔFosB, an immediate-early gene that persists for weeks to months (Nestler, 2008).

The transcription factor ΔFosB, a FosB splice variant lacking two PEST (P, proline; E, glutamic acid; S, serine; and T, threonine-rich) protein degradation sequences (Nestler, 1999), has been extensively investigated in the nucleus accumbens (Nestler, 2008) (Nestler, 2001). In the nucleus accumbens, increased ΔFosB levels results in increased motivation to seek artificial and natural rewards, such as cocaine, sucrose, running and sex (Kelz, 1999; Wallace, 2008; Werme, 2002). On the other hand, an insufficient increase in ΔFosB corresponds to reduced resilience in major depressive disorder (Vialou, 2010). Therefore, ΔFosB levels in the nucleus accumbens is proposed to set the degree of motivation in goal-directed behaviors (Vialou, 2010; Nestler, 1999). In contrast, the role of ΔFosB in the dorsal striatum is less known.

One gene that is regulated by ΔFosB is *Grin2b*, which encodes for GluN2B (also known as NR2B), an *N*-methyl-d-aspartate glutamate receptor (NMDAR) modulatory subunit (Grueter, 2013). GluN2B endows NMDARs with slow channel kinetics and the ability to bind to calcium/calmodulin-dependant kinase II (CaMKII), properties that influence $\alpha$-amino-3-hydroxy-5-methyl-4-isoxazolepropionic acid glutamate receptor (AMPAR) trafficking at dendritic spines (Zhou, 2007; Foster, 2010; Hall, 2007). In fact, GluN2B is critical for the formation and maintenance of silent synapses, immature synapses that express NMDARs but lack detectable AMPARs (Gray, 2011; Lee, 2010; Kerchner, 2008). Intriguingly, in *Sapap3*-null mice direct-pathway medium spiny neurons (D1 MSNs) contain more silent synapses (Wan Y., 2011).

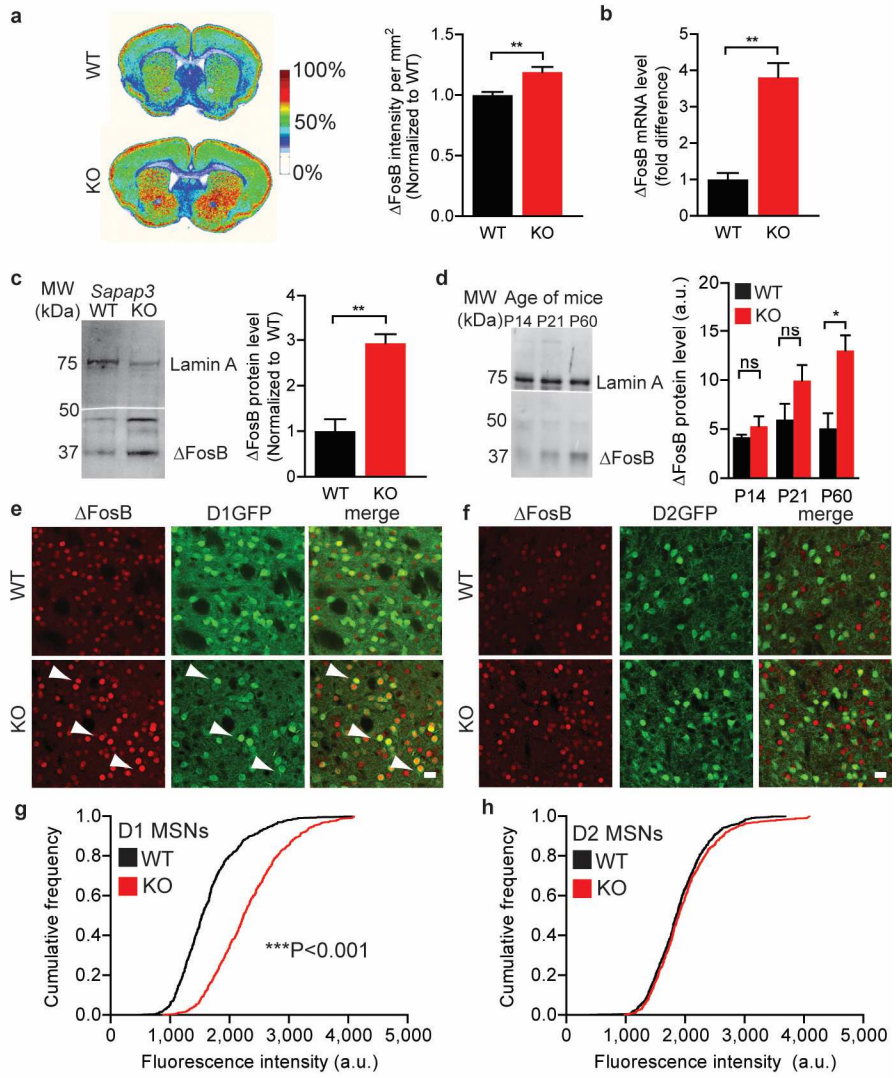


**Figure 5: Elevated ΔFosB in D1 MSNs of adult *Sapap3*$^{-/-}$ mice. a, Increased striatal FosB immunofluorescence in *Sapap3*$^{-/-}$ (KO) mice compared to wildtype (WT) littermates (n=6). b, Elevated striatal ΔFosB mRNA levels in *Sapap3*$^{-/-}$ mice (n=3). c, Higher striatal ΔFosB protein levels in *Sapap3*$^{-/-}$ mice (n=3). d, Striatal ΔFosB levels rises with age in postnatal day 14 (P14), P21 and P60 *Sapap3*$^{-/-}$ mice (n=3). e, f, FosB (red) co-localizes with D1GFP and D2GFP. g, No co-localization of FosB (red) with choline acetyltransferase (ChAT) or parvalbumin (PV), in green. h, i, Cumulative distribution graphs reveal increased FosB immunofluorescence in *Sapap3*$^{-/-}$ D1 MSNs, but not D2 MSNs (WT;D1GFP n=551, KO;D1GFP n=615, WT;D2GFP n=727, KO;D2GFP n=656 cells, 4 mice per group). **P<0.01, ***P<0.001, ns: not significant,**

**two-tailed unpaired *t* test (a-e), or two-sample Kolmogorov-Smirnov test (h, i). Scale bar: 10 μm. Graphs show means±s.e.m.**

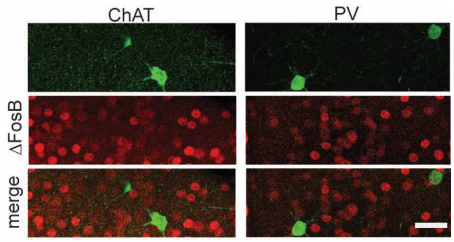


**Figure 6: ΔFosB is not expressed in striatal interneurons. No co-localization of ΔFosB (red) with choline acetyltransferase (ChAT) or parvalbumin (PV), in green. Scale bar: 10 μm.**

## *3.2 ΔFosB elevation in D1 MSNs of Sapap3 $^{-/-}$ mice*

To test whether mice homozygous for the Sapap3 deletion (*Sapap3*$^{-/-}$) exhibit hyperactivity in the cortico-striatal-thalamo-cortical loop like patients with OCD, we used FosB to label chronically perturbed neurons. Quantitative immunohistochemistry revealed significantly increased intensities of FosB immunofluorescence in the striatum of *Sapap3*$^{-/-}$ mice compared to wildtype littermates (Figure 5a). Furthermore, quantitative real-time PCR with reverse transcription (qRT-PCR) confirmed that transcription of the ΔFosB splice variant was upregulated in *Sapap3*$^{-/-}$ mice (Figure 5b). Correspondingly, Western blotting using striatal nuclear lysates showed elevated levels of ΔFosB, the spliceoform of FosB that persists for weeks to months after chronic perturbations, in *Sapap3*$^{-/-}$ mice (Figure 5c). To determine when ΔFosB levels became elevated, we probed for ΔFosB in striatal nuclear lysates of postnatal day 14 (P14), P21

and P60 *Sapap3*$^{-/-}$ mice using Western blotting. ΔFosB levels in the striatum of *Sapap3*$^{-/-}$ mice rose with age in *Sapap3*$^{-/-}$ pups, and reached a level significantly higher than wildtype littermates by P60 (Figure 5d). Therefore, the age when ΔFosB levels became significantly elevated corresponded with the age when compulsive grooming was first observed in *Sapap3*$^{-/-}$ mice. Interestingly, *Slitrk5*-null mice, another mouse model for OCD, also expressed heightened levels of striatal ΔFosB, suggesting that this phenomenon is not restricted to the *Sapap3*$^{-/-}$ mouse model (Figure 7).

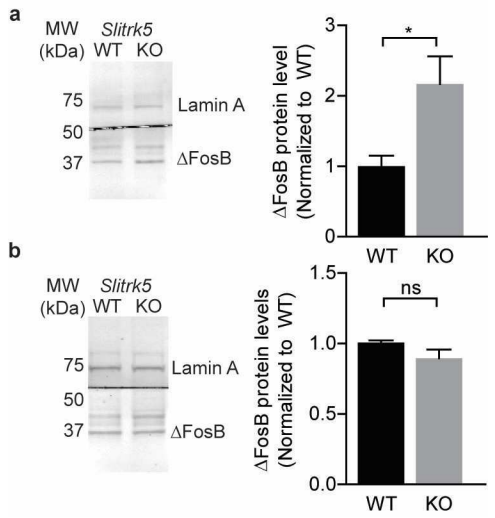


**Figure 7**: **Increased striatal ΔFosB expression in *Slitrk5*$^{-/-}$ mice. a, Western blot of nuclear extracts showing increased ΔFosB expression in the striatum of *Slitrk5*$^{-/-}$ mice (KO) compared to wildtype (WT) littermates (n=6). b, Western blot of nuclear extracts from the frontal cortex (including the orbitofrontal cortex) of *Slitrk5*$^{-/-}$ mice and wildtype littermates do not show a significant difference in ΔFosB levels (n=3). *P<0.05, ns: not significant, two-tailed unpaired *t* test. Graphs represent means and s.e.m.**

Approximately half of the medium spiny neurons (MSNs) in the striatum makes up the direct pathway and express dopamine 1a receptors (D1 MSNs), while the other half constitutes the indirect pathway and express dopamine 2 receptors (D2 MSNs). These two groups of MSNs are morphological identical and intermingled. To distinguish between direct and indirect-pathway MSNs, we generated *Sapap3*$^{-/-}$ mice that carry D1GFP and D2GFP bacterial artificial chromosome (BAC) transgenes. The D1GFP BAC transgene expresses enhanced green fluorescent protein (EGFP) under the control of the type 1a dopamine receptor promoter to label direct-pathway MSNs, while the D2GFP BAC transgene drives EGFP expression using the D2 dopamine receptor promoter to tag indirect-pathway MSNs (Gong, 2003). We found that FosB co-localized with D1 MSNs in *Sapap3*$^{-/-}$; D1GFP mice and D2 MSNs in *Sapap3*$^{-/-}$;D2GFP mice (Figure 5e, f). Conversely, there was no co-localization of FosB with parvalbumin (PV) or choline acetyltransferase (ChAT), markers for fast-spiking inhibitory interneurons and cholinergic interneurons, respectively (Figure. 6). Quantification of FosB immunofluorescence revealed that FosB levels were significantly higher in *Sapap3*$^{-/-}$ D1 MSNs, but not D2 MSNs (Figure 5g, h).

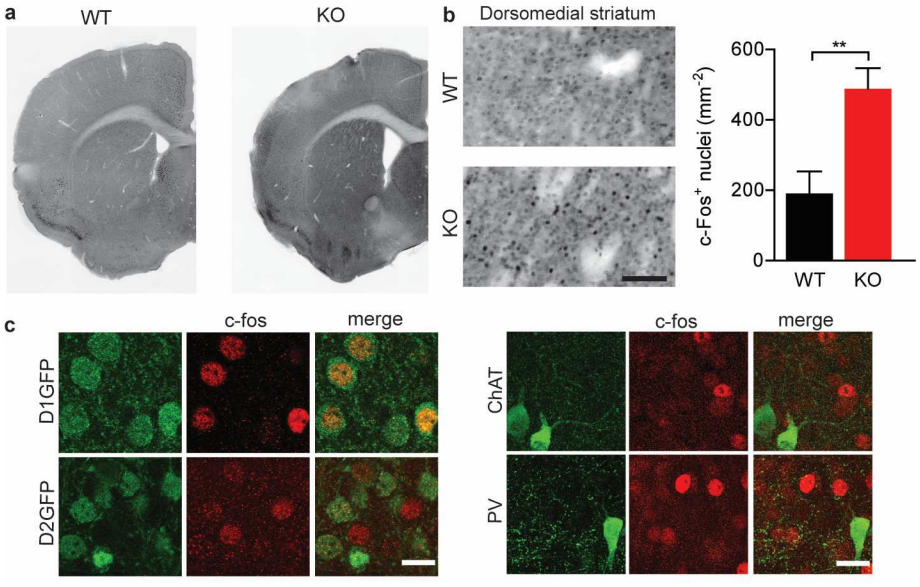


**Figure 8: Increased activation of dorsal striatum D1 MSNs during grooming in *Sapap3*$^{-/-}$ mice. a, More neurons activated (labeled with c-fos) in the dorsomedial striatum during grooming in *Sapap3*$^{-/-}$ (KO) mice compared to wildtype (WT) littermates. b, Higher magnification images of the dorsomedial striatum, and quantification of c-fos$^{+}$ nuclei in the dorsomedial striatum (n=6). Scale bar: 100 μm. c, Co-localization of c-fos (red) with D1GFP, but not D2GFP, parvalbumin (PV) or choline acetyltransferase (ChAT), in green, in *Sapap3*$^{-/-}$ mice. Scale bar: 10 μm. Scale bar: 100 μm. **P<0.01, two-tailed unpaired *t* test. Graphs show means±s.e.m.**

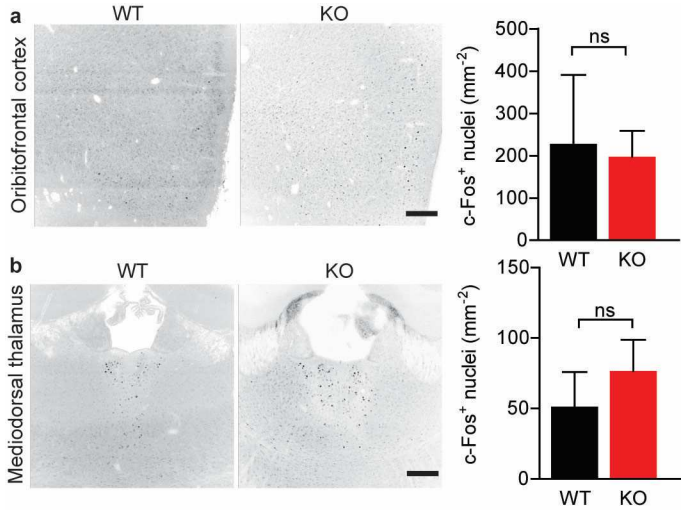


**Figure 9: Activation of orbitofrontal cortex and dorsomedial nucleus of the thalamus during grooming. a, Quantification of the density of c-fos$^+$ nuclei in the orbitofrontal cortex reveals no significant difference between *Sapap3*$^{-/-}$ (KO) and wildtype (WT) mice (n=6). b, Quantification of c-fos$^+$ nuclei in the mediodorsal nucleus of the thalamus showed no difference between *Sapap3*$^{-/-}$ and wildtype mice (n=6). Scale bar: 100 μm. ns: not significant, two-tailed unpaired *t* test. Graphs show means±s.e.m.**

## *3.3 Compulsive grooming activates more D1 MSNs*

To map the brain regions that exhibit abnormal activity during compulsive grooming in *Sapap3*$^{-/-}$ mice, we quantified the number of neurons expressing c-fos, a marker of acute neuronal activity, during grooming bouts in *Sapap3*$^{-/-}$ mice and wildtype littermates. In *Sapap3*$^{-/-}$ mice, compulsive grooming led to more c-fos$^+$ nuclei in the dorsomedial striatum (also known as the caudate), a brain region involved in the acquisition of action-outcome associations and formation of habits (Figure 8a, b) (Thorn, 2010; Ragozzino, 2007; Yin, 2006). In addition, we found that c-fos co-localized with D1

MSNs, but not ChAT, PV, or D2 MSNs in *Sapap3*$^{-/-}$ mice (Figure 8c). On the other hand, the densities of neurons activated in the orbitofrontal cortex and mediodorsal nucleus of the thalamus, two brain regions that send axonal projections to the dorsomedial striatum (Oh, 2014), were not significantly different between wildtype and *Sapap3*$^{-/-}$ mice (Figure 9). Therefore, in *Sapap3*$^{-/-}$ mice more dorsal striatum D1 MSNs, the cell type that expresses elevated levels of ΔFosB, are activated during compulsive grooming.

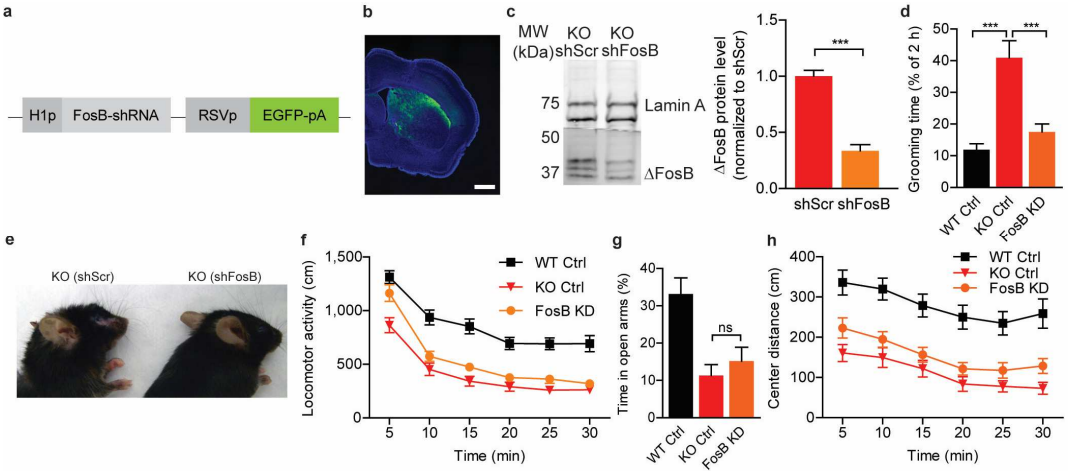


**Figure 10: Knock-down of FosB in the dorsal striatum rescues OCD-like behavior in *Sapap3*$^{-/-}$ mice. a, Schematic of vector expressing FosB shRNA and EGFP. b, EGFP is expressed in the dorsal striatum two weeks after viral injection. Scale bar: 1 mm. c, FosB shRNA (shFosB) reduces striatal ΔFosB levels by ~75% in *Sapap3*$^{-/-}$ (KO) mice, compared to control scrambled shRNA (shScr) (n=3, two-tailed unpaired *t* test). d, Reduced grooming time in *Sapap3*$^{-/-}$ mice injected with shFosB (FosB KD), compared to *Sapap3*$^{-/-}$ mice injected with control scrambled shRNA (KO Ctrl) (n=22). e, Disparate skin conditions of *Sapap3*$^{-/-}$ mice transduced with either shFosB (FosB KD) or control scrambled shRNA (KO Ctrl). f, Locomotor activity is not significantly altered (n=22). g, Time spent in the open arms of the zero maze is unaffected (n=22). h, Distance travelled at the center of the open field is not significantly changed (n=22). **P<0.01, ***P<0.001, ns: not significant, ANOVA with post-hoc Bonferroni test. Graphs display means±s.e.m.**

### *3.4 FosB knock-down rescues compulsive grooming*

Next we generated adeno-associated viruses (AAV) expressing FosB short hairpin RNA (shRNA) to investigate whether ΔFosB is required for the expression of OCD-like behavior. The AAV construct featured a FosB shRNA construct driven by a H1 promoter, and an enhanced green fluorescent protein (EGFP) transgene under the control of a Rous sarcoma virus (RSV) promoter (Figure 10a). We injected AAV expressing FosB shRNA (shFosB) or AAV expressing control scrambled shRNA (shScr) into the dorsal striatum of *Sapap3*$^{-/-}$ mice, and EGFP expression was observed two weeks after injection of the AAV (Figure 9b). Western blotting indicated that the FosB shRNA lowered ΔFosB levels by around 75% compared to the control scrambled shRNA (Figure 10c).

Two to three weeks after the viral injections, we conducted overnight video monitoring of the mice. We found that *Sapap3*$^{-/-}$ mice with AAV expressing FosB shRNA virus injected in the dorsal striatum spent markedly less time grooming compared to *Sapap3*$^{-/-}$ controls injected with AAV expressing scrambled shRNA (Figure 10d). As a result, all *Sapap3*$^{-/-}$ controls injected with scrambled shRNA developed characteristic skin lesions indicative of compulsive grooming, whereas *Sapap3*$^{-/-}$ mice treated with AAV expressing FosB shRNA did not exhibit skin lesions (Figure 10e). Locomotor activity of the mice was unaffected by the knock-down of FosB (Figure 10f). Likewise, anxiety-like behavior measured on the open field and zero maze tests were not affected by knock-

down of FosB (Figure 10g, h). Unlike *Sapap3*$^{-/-}$ mice, knock-down of ΔFosB in wildtype mice did not affect grooming times (Figure 11), which was expected since wildtype mice have low basal levels of ΔFosB.

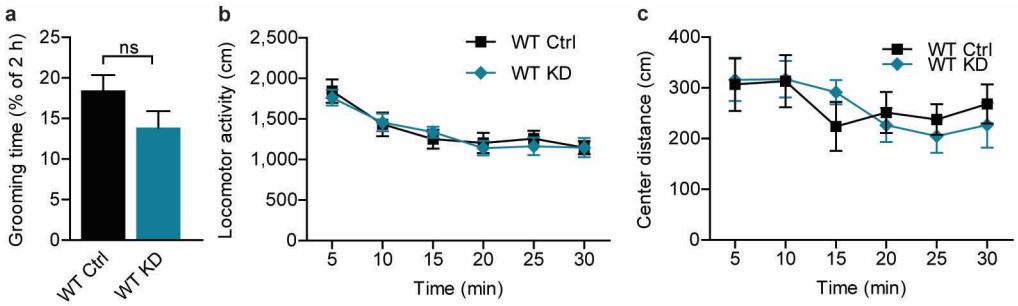


**Figure 11: Knock-down of ΔFosB in WT mice affects neither grooming nor locomotion. a, Grooming times of wildtype (WT) mice with ΔFosB knocked down in the dorsal striatum (WT KD) are not significantly different from WT mice injected with the scrambled shRNA control (WT Ctrl) virus (n=10). b, Locomotor activity is not significantly changed by knock-down of ΔFosB in wildtype mice (n=10). c, The distance moved at the center of the open field is unaltered by knock-down of ΔFosB in wildtype mice (n=10). ns: not significant, unpaired two-tailed *t* test. Graphs indicate means and s.e.m.**

## *3.5 Overexpression of ΔFosB increases grooming behavior*

To determine whether overexpression of ΔFosB is sufficient to increase grooming behavior, we injected AAV expressing ΔFosB-EGFP into the dorsal striatum of wildtype mice at postnatal day 21 (P21) to mimic the time course of ΔFosB accumulation in *Sapap3*$^{-/-}$ mice during neural development, and at 3 months old, when the brain is fully mature. Grooming behavior was measured when the mice were 4 months old. Interestingly, compared to wildtype littermates injected with EGFP control virus at P21, overexpression of ΔFosB in wildtype mice at P21 increased grooming behavior, while ΔFosB overexpression at 3 months old had no effect on grooming (Figure 12a).

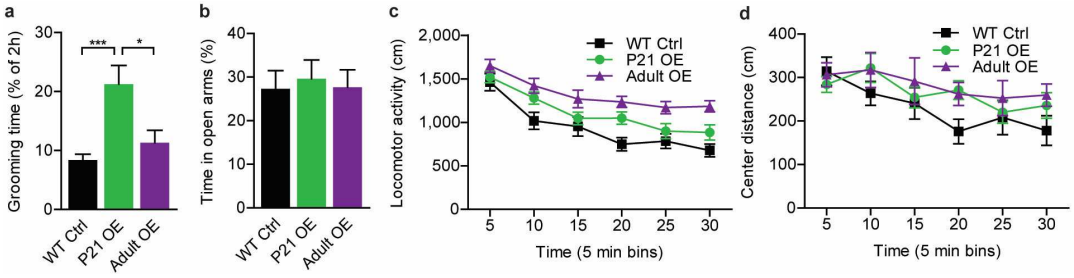


**Figure 12: Overexpression of ΔFosB in WT mice at P21 increases grooming behavior. a, Injection of adeno-associated virus (AAV) expressing the ΔFosB-EGFP overexpression vector into the dorsal striatum of wildtype mice (WT OE) at post-natal day 21 (P21), to mimic the time course of ΔFosB expression in *Sapap3*$^{-/-}$ mice, resulted in increased grooming times at 4 months old, compared to WT controls injected with AAV expressing the EGFP control vector (WT Ctrl) (n=14). In contrast, overexpression of ΔFosB-EGFP in 3 month old wildtype mice (Adult OE) did not alter grooming behavior at 4 months old (n=14). b, Time spent at the open arms of the zero maze was not affected by overexpression of ΔFosB (n=14). c, Locomotor activity was not changed by overexpression of ΔFosB (n=14). d, Distance travelled at the center of the open field was unaltered by ΔFosB overexpression (n=14). ***P<0.001, *P<0.05, ns: not significant, ANOVA with post-hoc Bonferroni test. Graphs show means and s.e.m.**

This result suggests that the developing brain is more vulnerable to perturbations that lead to compulsive behavior in adulthood, mirroring clinical studies linking childhood trauma to OCD and trichotillomania in adults (Lochner, 2002). In contrast, overexpression of ΔFosB had no significant effect on locomotor activity and anxiety-like behavior (Figure 12b-d), indicating that the increase in grooming behavior in wildtype animals was not due to changes in motor activity or anxiety. However, the grooming behavior in wildtype mice injected at P21, which groom for 20-30% of their time, is not as severe as knockout mice, which groom for 40-50% of their time. As a result, even though the wildtype mice injected with ΔFosB virus take 1-2 weeks longer for their surgical incisions to heal, they do not develop the characteristic hemorrhagic skin lesions seen in knockout mice. This suggests that overexpression of ΔFosB alone is not sufficient to generate the severe grooming phenotype seen in knockout mice, and that the lack of Sapap3 itself may exacerbate the cortico-striatal synaptic defect due to aberrant synapse maturation or homeostatic scaling.

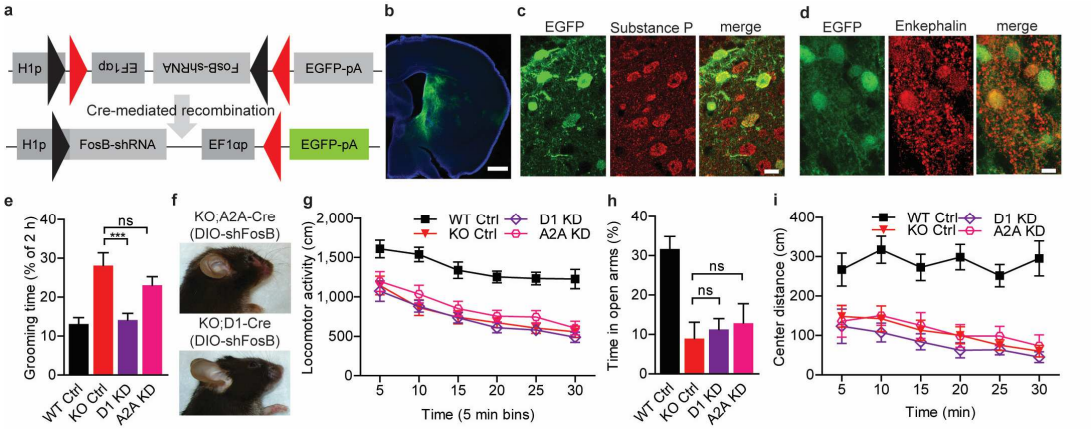


**Figure 13: Knock-down of FosB in dorsal striatum D1 MSNs alleviates OCD-like behavior in *Sapap3*$^{-/-}$ mice. a, Diagram of the DIO-shFosB cassette, which expresses FosB shRNA and EGFP after Cre-mediated recombination. Black triangles: TATA-loxP sites. Red triangles: lox2272 sites. b, EGFP expression in the dorsomedial striatum two weeks after viral injection. Scale bar: 1 mm. c, Co-localization of EGFP with Substance P in *Sapap3*$^{-/-}$;D1-Cre mice transduced with DIO-shFosB (D1 KD). Scale bar: 10 μm. d, Co-localization of EGFP with met-enkephalin in *Sapap3*$^{-/-}$;A2A-Cre mice transduced with DIO-shFosB (A2A KD). Scale bar: 10 μm. e, Reduced grooming time in *Sapap3*$^{-/-}$; D1-Cre mice injected with DIO-shFosB (D1 KD). f, Contrasting skin conditions of *Sapap3*$^{-/-}$;A2A-Cre and *Sapap3*$^{-/-}$; D1-Cre mice injected with DIO-shFosB. g, Locomotor activity is unchanged. h, Time spent in the open arms of the elevated zero maze is unaffected. i, Distance moved at the illuminated center of the open field chamber is unaltered. Wildtype mice injected with shScr (WT Ctrl) n=16, *Sapap3*$^{-/-}$ mice injected with shScr (KO Ctrl) n=16, *Sapap3*$^{-/-}$;D1-Cre injected with DIO-shFosB (D1 KD) n=15, *Sapap3*$^{-/-}$;A2A-Cre injected with DIO-shFosB (A2A KD) n=14. ***P<0.001, ns: not significant, ANOVA with post-hoc Bonferroni test. Graphs display means±s.e.m.**

### *3.6 FosB knock-down in D1 MSNs rescues compulsive grooming*

To dissect the cell type responsible for the OCD-like phenotype in *Sapap3*$^{-/-}$ mice, we engineered a novel Cre-inducible shRNA construct, DIOR (*D*ouble floxed *I*nverted *O*pen reading frame for small nuclear *R*NAs), that permitted the transcription of both FosB shRNA and EGFP after Cre-mediated recombination (Figure 13a). We injected AAV expressing the DIO-FosB shRNA construct into *Sapap3*$^{-/-}$;D1-Cre and *Sapap3*$^{-/-}$;A2A-Cre mice to knock down FosB specifically in direct-pathway MSNs and indirect-pathway MSNs, respectively (Figur 13b). EGFP expression was specific to medium spiny neurons expressing Substance P, a marker for D1 MSNs, in *Sapap3*$^{-/-}$;D1-Cre mice injected with the DIO-FosB shRNA construct (Figure 13c). Conversely, EGFP co-localized with met-enkephalin, a marker of D2 MSNs, in *Sapap3*$^{-/-}$;A2A-Cre mice injected with AAV expressing DIO-FosB shRNA (Figure 13d).

The *Sapap3*$^{-/-}$;D1-Cre mice injected with AAV expressing DIO-FosB shRNA spent significantly less time grooming compared to *Sapap3*$^{-/-}$ controls (Figure 13e). In contrast, knock-down of FosB in indirect-pathway MSNs resulted in a non-significant reduction compulsive grooming (Figure 13e). Consequently, whereas most *Sapap3*$^{-/-}$ mice with FosB knocked down in D2 MSNs (10 out of 14 mice) exhibited the severe ulcerative skin lesions characteristic of compulsive grooming, *Sapap3*$^{-/-}$ mice with FosB knocked down specifically in D1 MSNs did not develop skin lesions (Figure 13f). Locomotor activity and anxiety-like behavior measured in the open field and elevated zero maze tests,

however, were not altered by knock-down of FosB specifically in D1 or D2 MSNs (Fig. Figure 13g-i).

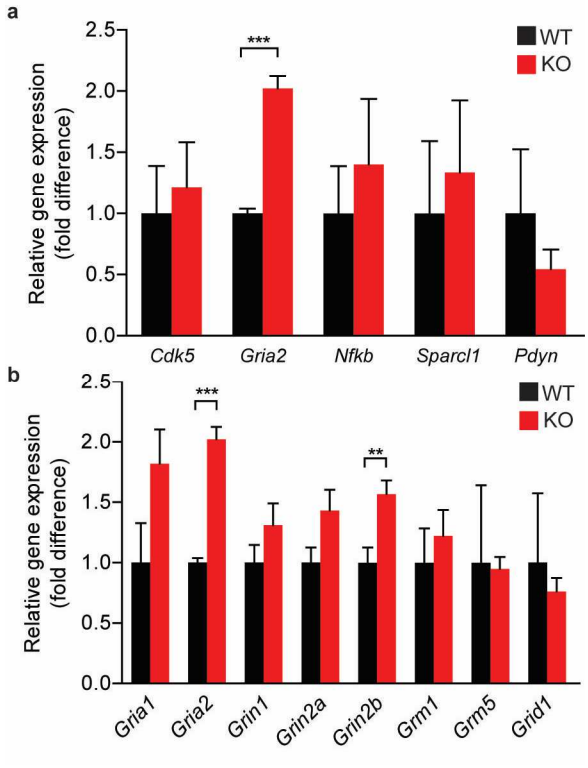


**Figure 14: Extended qRT-PCR results. a, Messenger RNA (mRNA) levels of selected ΔFosB gene targets previously published, assessed by quantitative real-time PCR with reverse transcription (qRT-PCR) using striatal tissue from adult *Sapap3*$^{-/-}$ mice (KO) and wildtype (WT) littermates (n=6). b, Striatal mRNA levels of selected genes that encode for components of glutamate receptors, determined using qRT-PCR (n=6). **P<0.01, ***P<0.001, two-tailed unpaired *t* test. Graphs indicate means and s.e.m.**

## 3.7 ΔFosB upregulates GluN2B expression

Since ΔFosB affects the expression of multiple genes (Nestler, 2001), we expected to observe dysregulation of gene expression in *Sapap3*$^{-/-}$ mice. To identify genes that were dysregulated in the dorsal striatum of *Sapap3*$^{-/-}$ mice, we used qRT-PCR to determine the mRNA levels of previously published ΔFosB gene targets and postsynaptic glutamate receptors (Figure 14). We found that *Grin2b* transcription was significantly upregulated in *Sapap3*$^{-/-}$ mice (Figure 15a).

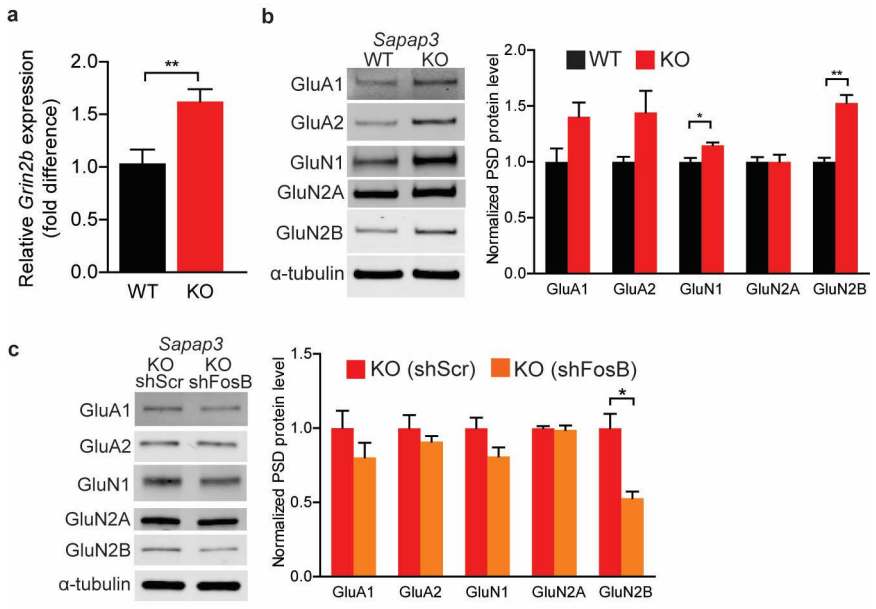


**Figure 15: Knock-down of FosB reduces excessive GluN2B expression in *Sapap3*$^{-/-}$ mice. a, Quantitative real-time PCR with reverse transcription (qRT-PCR) reveals increased striatal expression of *Grin2b* in *Sapap3*$^{-/-}$ (KO) mice (n=6) compared to wildtype (WT) littermates. b, Increased GluN2B protein levels in striatal post-synaptic densities (PSD) of *Sapap3*$^{-/-}$ mice (n=3). c, Knock-down of FosB (shFosB) reduces GluN2B levels in striatal PSD of *Sapap3*$^{-/-}$ mice, compared to control scrambled shRNA (shScr) (n=3). Graphs represent means±s.e.m. *P<0.05, **P<0.01, two-tailed unpaired *t* tests.**

To assess the level of GluN2B at striatal synapses, we isolated post-synaptic density (PSD) fractions from striatal lysates of adult *Sapap3*$^{-/-}$ and wildtype littermates and ran the PSD fractions on Western blots. We found that GluN2B protein levels were significantly elevated in the PSD of *Sapap3*$^{-/-}$ mice (Figure 15b). Correspondingly, knock-down of ΔFosB by AAV expressing FosB-shRNA resulted in a significant reduction in GluN2B levels in the PSD of striatal excitatory synapses of *Sapap3*$^{-/-}$ mice (Figure 15c). In contrast, expression of *Grin2a*, which encodes another NMDAR modulatory subunit, was not significantly altered in *Sapap3*$^{-/-}$ mice (Figure 14b).

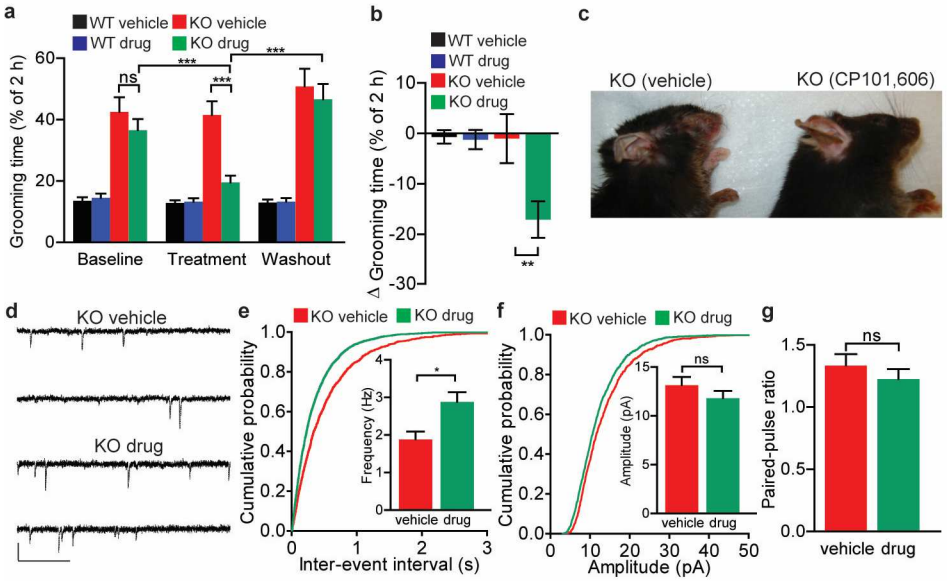


**Figure 16: GluN2B antagonism rescues compulsive grooming and synaptic defect in *Sapap3*$^{-/-}$ mice. a, Treatment with CP101,606 reduces grooming times in *Sapap3*$^{-/-}$ mice, and compulsive grooming resumes after washout of the drug (n=20). b, Greater reductions in grooming times in *Sapap3*$^{-/-}$ mice treated with CP101,606 (n=20). ANOVA with post-hoc Bonferroni test for comparison between multiple groups or two-tailed paired *t* test for comparison of changes in individual mice (a,b). c, Disparate appearances of *Sapap3*$^{-/-}$ mice treated with either vehicle or CP101,606. d, Representative traces of miniature excitatory postsynaptic currents (mEPSCs) recorded from *Sapap3*$^{-/-}$ (KO) D1 MSNs incubated with either CP101,606 (drug) or vehicle. Scale bars: 20 pA and 500 ms. e, Frequency of mEPSCs recorded from *Sapap3*$^{-/-}$ D1 MSNs is significantly increased by perfusion with CP101,606 (n=8 WT, 10 KO cells, 4 mice per group). f, Amplitude of mEPSCs is not altered by CP101,606 (n=8 WT, 10 KO cells, 4 mice per group). g, Paired-pulse ratio is unchanged by CP101,606 (n=10 WT, 12 KO cells, 3 mice per group). Two-tailed unpaired *t* test (e-g). *P<0.05, **P<0.01, ***P<0.001, ns: not significant, Graphs indicate means±s.e.m.**

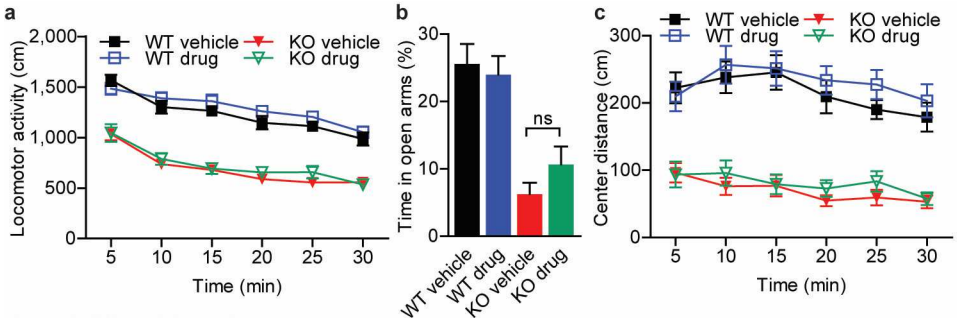


**Figure 17: CP101,606 does not alter anxiety-like behavior. a, Locomotor activity in the open field is unchanged by CP101,606 (n=20). b, Time spent in the open arms of the zero maze is unaffected by CP101,606 (n=20). c, CP101,606 does not change the distance travelled at the center of the open field (n=20). ns: not significant, ANOVA with post-hoc Bonferroni test. Graphs indicate means±s.e.m.**

## *3.8 GluN2B inhibition rescues physiology and behavior*

Finally, to determine if the upregulation of GluN2B is relevant to compulsive grooming in *Sapap3*$^{-/-}$ mice, we treated *Sapap3*$^{-/-}$ mice and wildtype littermates with CP101,606, a highly specific antagonist of GluN2B-containing NMDARs. After drug administration, *Sapap3*$^{-/-}$ mice treated with CP101,606 spent significantly less time grooming compared to *Sapap3*$^{-/-}$ littermates treated with vehicle, and grooming times returned to elevated levels after washout of the drug (Figure 16a, b). As a result, 11 out of 20 *Sapap3*$^{-/-}$ controls treated with vehicle developed ulcerative skin lesions during two weeks of treatment with the vehicle, while only 2 out of 20 *Sapap3*$^{-/-}$ littermates treated with CP101,606 mesylate exhibited skin lesions during the treatment period (Figure 16c). Conversely, anxiety-like behavior and locomotor activity were not significantly altered by CP101,606 (Figure 17a-c).

*Sapap3*$^{-/-}$ D1 MSNs manifest diminished excitatory synaptic transmission through a reduction in the frequency of miniature excitatory postsynaptic currents (mEPSCs), the consequence of an increased proportion of silent synapses (Welch, 2007; Wan Y., 2011). To determine whether upregulation of *Grin2b* contributes to this synaptic defect, we used whole-cell patch-clamp electrophysiology to measure the effect of CP101,606, a GluN2B antagonist, on *Sapap3*$^{-/-}$ D1 MSNs in acute brain slices. Perfusion with CP101,606 resulted in a significant increase in mEPSC frequency in *Sapap3*$^{-/-}$ D1 MSNs and D2 MSNs (Figure 16d, e, Figure 19). In contrast, mEPSC amplitude (normal in *Sapap3*$^{-/-}$ mice) was unaffected by CP101,606, indicating that the drug did not recruit more AMPARs to existing mature synapses (Figure 16f, Figure 19). In addition, the paired-pulse ratio (PPR) recorded from *Sapap3*$^{-/-}$ D1 MSNs was not significantly changed by CP101,606 perfusion, implying that the drug did not affect presynaptic release probability (Figure 16g). As expected, CP101,606 treatment did not affect mEPSC amplitude or frequency in wildtype D1 and D2 MSNs (Figure 18, Figure 19), suggesting that the effect is specific to *Sapap3*$^{-/-}$ MSNs. Thus, our electrophysiological results suggest that GluN2B antagonism restores excitatory synaptic transmission in *Sapap3*$^{-/-}$ D1 MSNs by lowering the percentage of immature silent synapses. Taken together, our results demonstrate that ΔFosB-mediated upregulation of *Grin2b* in dorsal striatum D1 MSNs is required for OCD-like behavior in *Sapap3*$^{-/-}$ mice.

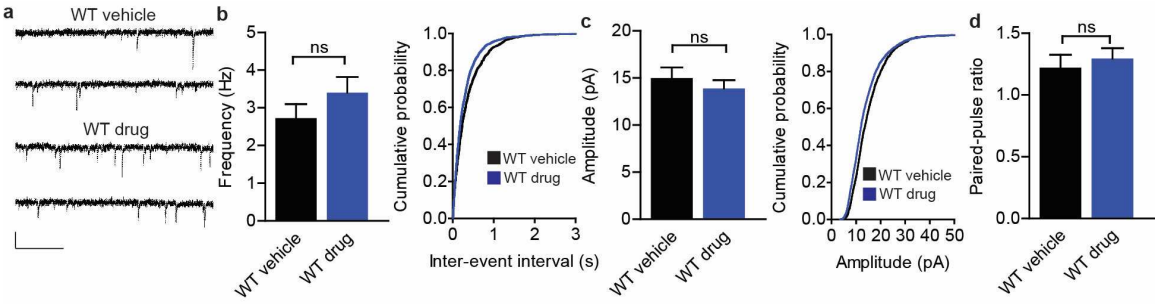


**Figure 18: GluN2B antagonism does not affect excitatory synaptic transmission in wildtype D1 MSNs. a, Representative traces of miniature excitatory postsynaptic currents (mEPSCs) recorded from wildype (WT) direct-pathway medium spiny neurons (D1 MSNs) incubated with CP101,606 (drug) or artificial cerebrospinal fluid (vehicle). Scale bars: 20 pA, 500 ms. b, mEPSC frequency is not significantly altered by CP101,606 (n=6 cells for vehicle, 11 for drug, 4 mice per group). c, mEPSC amplitude is not significantly changed by CP101,606 (n=6 for vehicle, 11 for drug, 4 mice per group). d, The paired-pulse ratio was unaltered by CP101,606 incubation (n=8 for vehicle, 7 for drug, 3 mice per group). ns: not significant, two-tailed unpaired *t* test. Graphs show means and s.e.m.**

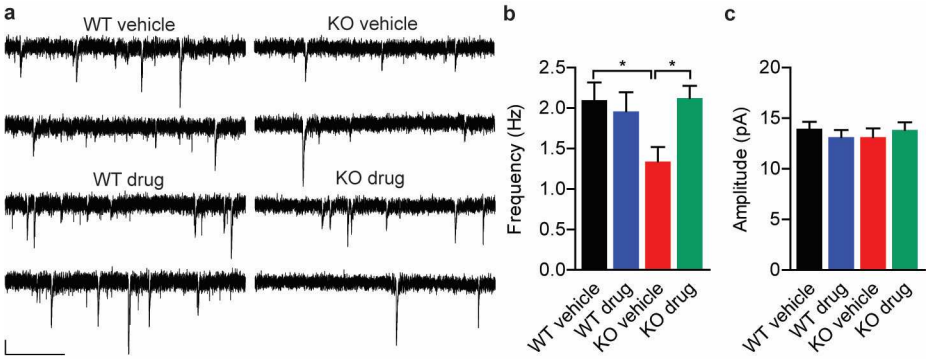


**Figure 19: GluN2B antagonism rescues excitatory synaptic transmission in *Sapap3*$^{-/-}$ D2 MSNs. a, Representative traces of miniature excitatory postsynaptic currents (mEPSCs) from wildtype (WT) and *Sapap3*$^{-/-}$ (KO) indirect-pathway medium spiny neurons (D2 MSNs) after incubation in CP101,606 (drug) or artificial cerebrospinal fluid (vehicle). Scale bars: 5 pA, 500 ms. b, CP101,606 rescues mEPSC frequency in *Sapap3*$^{-/-}$ (KO) D2 MSNs. c, CP101,606 has no effect on mEPSC amplitude. n=15 cells for WT vehicle, 11 for WT drug, 13 for KO vehicle, 14 for KO drug, 3 mice per group, *P<0.05, ANOVA with post-hoc Bonferroni test. Graphs display means and s.e.m.**

## 3.9 Discussion

Our results dovetail with previously published observations regarding ΔFosB and clinical findings in patients with OCD. Environmental factors that increase ΔFosB in the striatum are also associated with OCD. For instance, chronic stress increases ΔFosB levels in MSNs in rodents, and correspondingly, stress is known to exacerbate obsessions and compulsions in patients suffering from OCD (Perrotti, 2004; Gershuny, 2008; Nacasch, 2011). Likewise, cocaine use, which increases ΔFosB levels in both the nucleus accumbens and dorsal striatum, is a risk factor for OCD (Nestler, 2001; Crum, 1993).

Abnormal glutaminergic transmission at NMDARs is proposed to mediate OCD symptoms (Pittenger, 2011). Human genetic studies have found associations between OCD diagnoses and variants of the GluN2B gene at the three prime untranslated region (3'-UTR), a region important for mRNA transcript stability and translation (Arnold, 2004) (Alonso, 2012). Moreover, preliminary studies using NMDAR antagonists such as memantine and ketamine have shown promise in the alleviation of OCD symptoms (Stewart, 2010; Aboujaoude, 2009; Rodriguez, 2011). These studies augur well with our findings and support the identification of GluN2B as a novel therapeutic target for OCD. Indeed, further research is warranted to decipher the sources of aberrant synaptic inputs to D1 MSNs that lead to ΔFosB and GluN2B elevations, and to establish whether our findings translate to efficacious therapies for patients.

# Chapter 4: Discussion

As with any scientific study, answering one question often leads to more questions. Many pertinent questions have arisen from this project. Why does ΔFosB increase in *Sapap3*-mutant medium spiny neurons? Why is there increased firing in *Sapap3*-mutant medium spiny neurons at baseline and during compulsive grooming when cortico-striatal transmission is reduced, and how is this related to upregulation of GluN2B? Why is anxiety-like behavior not rescued with striatal knock down of FosB? These are interesting questions that warrant further discussion and investigation.

## *4.1 Mechanism of ΔFosB elevation*

What causes ΔFosB elevation in medium spiny neurons? Salient stimuli like chronic stress, such as chronic restraint stress or social defeat stress, drugs of abuse, such as cocaine and amphetamines, and dopamine agonists, like levodopa, can increase ΔFosB in direct-pathway medium spiny neurons. It is also known that FosB transcription can be driven by phosphorylated CREB, which is in turn phosphorylated by the PKA and Ras/MEK/ERK pathways. Since Ras/MEK/ERK signaling can be triggered by calcium influx into the cell, it follows that increased intracellular calcium concentration plays a key role in increased ΔFosB levels in medium spiny neurons.

What is the source of calcium influx in the medium spiny neuron? Three leading candidate are the L-type voltage-gated calcium channel (Simms, 2014), the inositol 1,4,5-triphosphate receptor (IP3R) (Choe, 2006), and the ryanodine receptor (RyR) (Taylor, 2010). The L-type voltage-gated calcium channel is located at the soma and proximal dendrites to influence gene expression, especially of immediate-early genes like FosB. The high baseline firing rates of *Sapap3*-null medium spiny neurons are likely to result in greater calcium influx through voltage-gated L-type calcium channels. On the other hand, IP3R and RyR are located on the endoplasmic recticulum (ER). These receptors are coupled to the L-type calcium channels, and therefore release intracellular calcium during the high baseline activity of the medium spiny neurons, leading to the phosphorylation of CREB and FosB transcription.

## *4.2 Mechanism of striatal hyperactivity*

The mechanism of striatal hyperactivity at baseline and during symptom provocation in *Sapap3*-mutant mice is unknown. There are four possible explanations for the hyperactivity observed: a decrease in local inhibition by inhibitory interneurons, an increase in excitability of the medium spiny neuron, a "network effect" due to a dysfunction in indirect-pathway medium spiny neurons, or an increase in thalamo-striatal input to the medium spiny neuron.

First, there could be a reduction in local inhibitory input to the medium spiny neurons. Immunohistochemical experiments have indicated that there are fewer parvalbumin-expressing interneurons in the striatum of *Sapap3*-knockout mice (Burguiere, 2013), suggesting that there would be reduced inhibition on medium spiny neurons, leading more action potential firing. However, it is not known if this finding has a functional consequence. To answer this question, we would need to measure the inhibitory post-synaptic currents (IPSC) on medium spiny neurons to determine if there is indeed a functional reduction in inhibition on the cell.

Second, there could be a compensatory increase in the excitability of the medium spiny neuron. Due to a reduction in cortico-striatal inputs, the medium spiny neuron could change its membrane properties, such as by upregulation of voltage-gated calcium channels. In order to investigate this possibility, we would need to measure the intrinsic

membrane properties of the medium spiny neuron to determine if there is indeed a change in membrane excitability.

Third, there could be a "network effect". The indirect-pathway medium spiny neurons (D2 MSNs) inhibit activity in the cortico-striato-thalamo-cortical (CSTC) circuit. Therefore, a defect in D2 MSNs can result in a reduction in inhibition on the activity of this circuit, leading to CSTC hyperactivity. It is worth noting that Sapap4 is expressed at thalamo-striatal synapses, so medium spiny neurons can still be activated by thalamic input, despite the defect at cortico-striatal synapses (Wan, 2014). To test this hypothesis, we can use *Sapap3* conditional knock-in (cKI) and conditional knock-out (cKO) mice, crossed to A2A-Cre mice. If the lack of Sapap3 in D2 MSNs can lead to CSTC circuit hyperactivity, we would expect Sapap3-cKO ; A2A-Cre mice to develop compulsive grooming, since a defect in D2 MSNs should be sufficient to cause CSTC circuit hyperactivity. Conversely, we would expect Sapap3-cKI ; A2A-Cre mice to have normal grooming behavior, since normal function of D2 MSNs should be sufficient to rescue compulsive grooming behavior.

Fourth, there could be increased thalamo-striatal input to medium spiny neurons. Since thalamo-striatal synapses express Sapap4 and are functionally normal in Sapap3-mutant mice, and ΔFosB-mediated upregulation of GluN2B would promote LTP at these synapses, we might observe an increase in thalamo-striatal excitation of medium spiny neurons. Therefore, in the competition between thalamo-striatal and cortico-

striatal synapses at the medium spiny neuron, the thalamo-striatal synapses would win. This would result in hyperactivity of the thalamo-striatal circuit during compulsive behavior, bypassing cortical modulation on the cortico-striatal-thalamo-cortical circuitry. Thalamo-striatal connections are believed to deliver "bottom-up" signals encoding attention and arousal toward salient information, while the cortico-striatal circuit is believed to deliver "top-down" signals encoding information on action selection based on cognition (Kimura, 2004). As a result, salient stimuli would override cognitive, reward contingency-based action selection, potentially leading to compulsive behaviors.

To test this hypothesis, we can use in vivo recordings coupled with optogenetics. Stimulation of the thalamo-striatal pathway during grooming induced by spraying water on the head of the mouse should lengthen the grooming times, due to increased saliency of the stimuli. In addition, inhibition of the cortico-striatal pathway should also result in increased grooming times. By contrast, acute inhibition of the thalamo-striatal pathway or acute activation of the cortico-striatal pathway in *Sapap3*-mutant mice should alleviate compulsive grooming by reducing the saliency of the stimuli. It is also worth testing if this effect is specific to stimulation of specific cell types (such as D1 or D2 MSNs), by using Cre-mediated expression of channelrhodopsin (ChR2) or halorhodopsin (NpHR) coupled with wheat germ agglutin (WGA).

## *4.3 Mechanism of generalized anxiety*

One of the unexpected findings in the study was the inability to rescue anxiety-like behavior by knocking down FosB, because it was thought that the two behaviors are linked. Subsequently, there have been studies that demonstrate that compulsive behaviors and anxiety are distinct: Neural manipulations can increase stereotypic behaviors while reducing anxiety-like behavior (Dietrich, 2015). Moreover, reintroduction of Sapap3 at P7 can alleviate anxiety-like behavior, while adult overexpression of Sapap3 does not, suggesting that an irreversible event during neurodevelopment mediates the pathogenesis of generalized anxiety (Welch, 2007). Taken together, anxiety-like behavior is likely mediated by a circuit (separate from the cortico-striato-thalamo-cortical circuit) that is profoundly affected by events during neurodevelopment.

In the appendix, I show a preliminary experiment that maps the anxiety circuitry activated by a 5 minute-exposure to the open arm of the elevated zero maze. *Sapap3*$^{-/-}$ mice were left on the open arm of an elevated zero maze, and c-fos+ nuclei were used as a measure of neuronal activation during anxiety. Increased activation of the anterior cingulate cortex, basolateral amygdala and nucleus accumbens/central amygdala were observed. The brain circuit linking these three brain regions has been extensively studied (Peters, 2009). Cortical projection neurons send excitatory synaptic connections to inhibitory interneurons (intercalated neurons) that inhibit the basolateral amygdala-

to-central amygdala/nucleus accumbens connection. In situ hybridization has shown that Sapap3 is also expressed in the lateral amygdala (which is considered a cortical structure). Therefore, it might be possible that the projection from the cingulate cortex to the intercalated cells of the basolateral amygdala is impaired in *Sapap3*-null mice.

Inhibitory interneurons, such as parvalbumin interneurons, begin to die during the first postnatal week of neurodevelopment if they lack synaptic activity (Close, 2012). Immediate-early genes like Stab1 are crucial for cortical interneuron survival in early neurodevelopment, so it is possible that basolateral amygdala interneurons that lack Sapap3 would not survive during neuronal development, resulting in the hyperactivation of the basolateral amygdala-central amygdala circuit during anxiety-provoking events. To study this possibility, we would need to use field recordings to measure the cortico-basolateral amygdala population spike, to determine if it is abnormal in *Sapap3*$^{-/-}$ mice. Another way forward would be to label intercalated cells using transgenic Cre-lines, to determine if these cells have reduced survival during neuronal development. Of course, re-introduction of Sapap3 in the intercalated cells in knockout mice (either germline expression using conditional knock-in mice or viral overexpression before P7) should rescue anxiety-like behavior in these mice.

# Chapter 5: Appendix

## *5.1 Mapping of the anxiety circuitry in Sapap3-null mice*

While compulsive behavior was rescued by knock-down of FosB, anxiety-like behavior was not affected. This lead to the hypothesis that a different brain circuit is involved in generalized anxiety. Therefore, preliminary studies were done to map this brain circuitry in *Sapap3*-null mice.

### 5.1.1 Brain regions acutely activated by anxiety

In order to determine the brain regions involved in anxiety, I investigated c-Fos expression in knockout and wildtype mice after exposure to an anxiety-inducing stressor. A five-minute exposure to the open arm of the zero maze was chosen as a mild anxiety-like stressor. Two hours after exposure to the open arm, the mice were sacrificed, perfused and their brains were harvested for sectioning coronally and saggitally at fifty microns. Control mice were also separated into individual cages one hour before perfusion, but were not exposed to the open arm. Brain regions that exhibit an increase in c-Fos expression following exposure to the stressor include the cingulate cortex, nucleus accumbens, basolateral amygdala and hypothalamus. The results are consisent with fMRI studies in human subjects, and they are also congruent with previous studies on anxiety in mice. Importantly, the results reinforce the importance of

the ventral axis, also known as the limbic cortico-striato-thalamo-cortico loop, in anxiety. The number of c-Fos immunoreactive nuclei in both the wildtype and the knockout are similar; thus, chronic, rather than acute, activation of the anxiety circuitry might underlie the anxiety-like behavior in the *Sapap3*$^{-/-}$ mice.

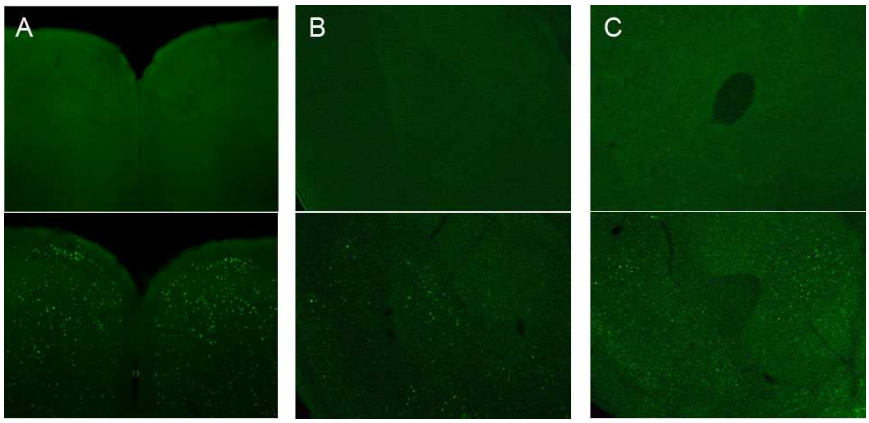


**Figure 20: c-Fos expression after exposure to elevated open arm for 5 minutes. Compared to controls that were not exposed to the mild stressor (above), *Sapap3*$^{-/-}$ mice that were exposed (below) exhibited c-Fos expression in areas such as the cingulate cortex (A), the basolateral amygdala (B) and the ventral striatum (C).**

### 5.1.2 Types of neurons acutely activated during anxiety

In order to determine the type of neurons that are activated in the cortex by open-arm exposure, I combined c-Fos immunohistochemistry with immunostaining for two neuronal markers, CaMKII and glutamic acid decarboxylase 67 (GAD67). CaMKII is a useful marker for non-GABAergic, noncholinergic, nonmonominergic excitatory neurons in the cortex, and it labels both pyramidal neurons and smaller, nonpyramidal

neurons of the cortex (Ouimet, 1984) (Fukunaga, 1988; Ochiishi T., 1994; Jones, 1994). On the other hand, GAD67 is a marker for inhibitory interneurons in the cortex. From the experiment, I observed that most of the Fos-immunoreactive cells in the anterior cingulate cortex express CaMKII instead of GAD67, and the results were similar for wildtype and knockout mice. Higher levels of c-Fos expression was also observed in the excitatory neurons in layer 2/3 compared to the other layers. The results show that during anxiety, excitatory principal neurons in the anterior cingulate cortex are activated, especially layer 2/3 pyramidal neurons that project intracortically to areas such as layer 5.

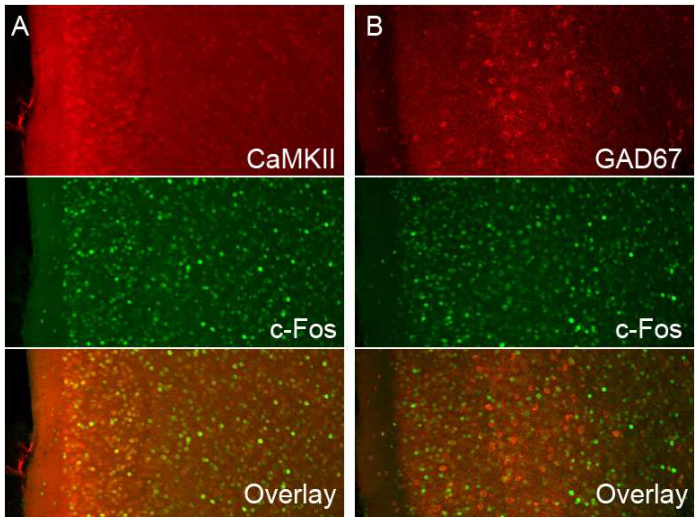


**Figure 21: Excitatory projection neurons in the anterior cingulate cortex, but not inhibitory interneurons, are activated during open-arm exposure. CaMKII immunolabelled excitatory projetion neurons in layers 2/3 and layer 5 have significant colocalization with c-Fos immunoreactive nuclei (A). In contrast, GAD67-labelled inhibitory interneurons in layer 4 do not have c-Fos immunoreactive nuclei (B).**

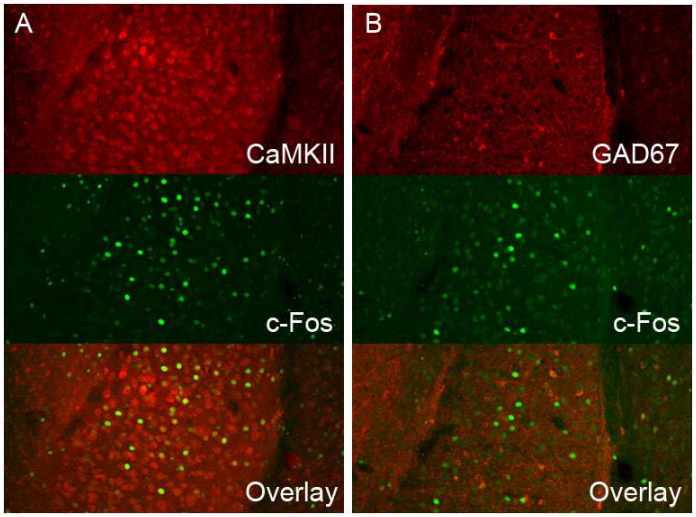


**Figure 22: Excitatory projection neurons in the basolateral amygdala are activated during open-arm exposure. CaMKII -immunolabelled neurons in the basolateral amygdala show greater c-Fos expression (A) compared to inhibitory interneurons expressing GAD67 (B).**

Similarly, in the basolateral amygdala, the Fos-immunoreactive nuclei also colocalize with CaMKII instead of GAD67, which suggests that the excitatory projection neurons from the amygdala are preferentially activated during anxiety-inducing stimuli.

## *5.2 Novel strategy for labeling cells before and after Cre recombination*

One unsolved question from our project is: Which cell types express Sapap3? Even though in situ hybridization studies have shown robust cortical, striatal and thalamic expression of Sapap3 mRNA, the exact cell types that express Sapap3 remain unknown. Another question that is pertinent is: Which cell type is Sapap3 required for compulsive behavior or anxiety-like behavior? To answer these questions, I designed a novel construct that can label cells where Sapap3 is conditionally knocked out or knocked in by Cre recombination.

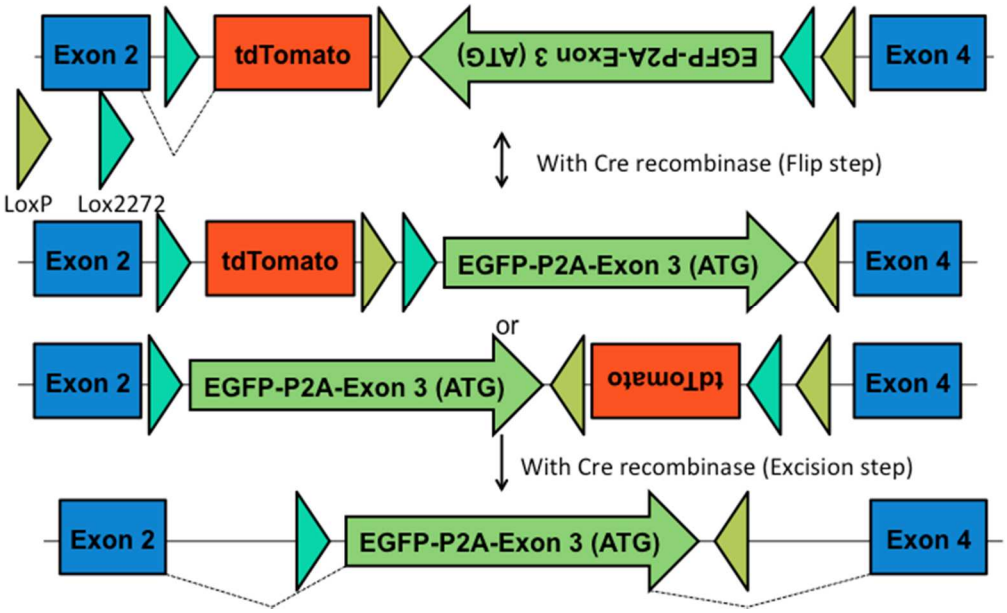


**Figure 23: Strategy for labeling cells before and after Cre recombination**

This novel construct would allow the *Sapap3*-expressing cells to be labeled with tdTomato before Cre-recombination, and EGFP after recombination. Therefore, it would

also allow the quantification of the efficiency of Cre-mediated recombination. Conversely, another similarly designed construct will allow the Cre-mediated knock out and labeling of neurons as well. However, the main limitation of this strategy is the difficulty in cloning the construct, and also there are difficulties involved in genotyping given its complexity. Therefore, this strategy might be more amenable for use in viral vectors instead, especially in cases where the efficiency of both infection and Cre-mediated expression of a construct needs to be ascertained. This strategy can also be used to identify select populations of cells that have undergone Cre-mediated recombination.

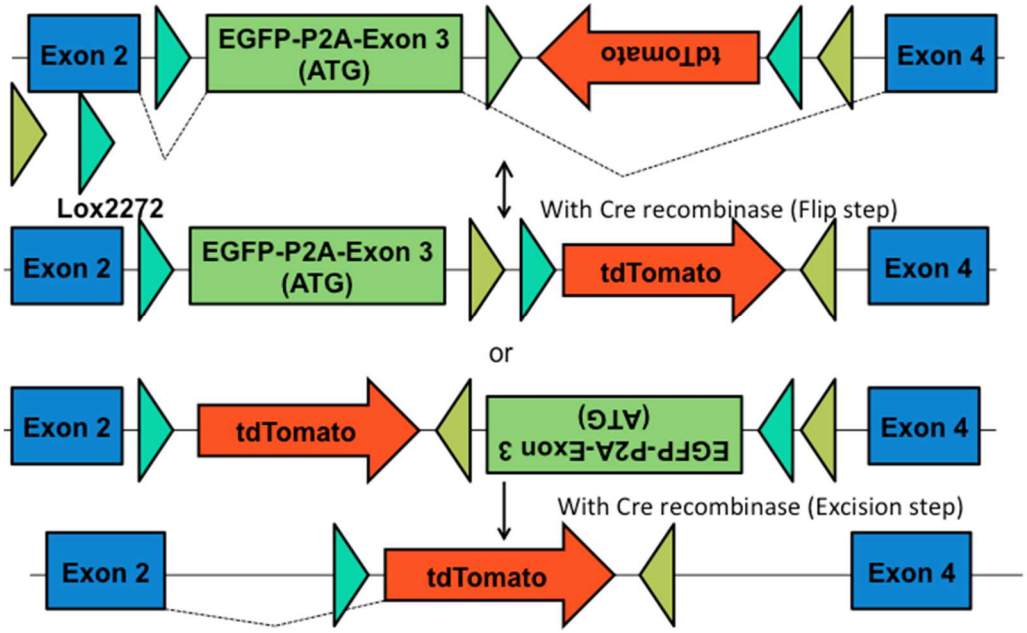


**Figure 24: Strategy to determine efficiency of conditional knock out of gene**

## *5.3 Novel strategy for labeling cells that express shRNA*

Another novel strategy that was introduced during the study is a novel way to label cells that express shRNA (Figure 13, 20): Double Inverted Open reading frame for short nuclear RNAs (DIOR). There are already strategies available to label cells that are transfected with a Cre-dependent shRNA but do not undergo Cre-recombination (Ventura, 2004): This usually involves inserting a EGFP cassette flanked by Cre sites in between the U6 promoter and the shRNA, and uses the knowledge that the U6 promoter must be directly proximal to the shRNA for transcription of the shRNA. This strategy also involves modifying the U6 promoter to incorporate a loxP site (called a TATA-loxP since the loxP site is embedded in a TATA box). In order to generate the novel construct that labels cells expressing shRNA after Cre recombination, I combined two concepts: the Double-floxed Inverted Open reading frame (DIO) concept of using two pairs of loxP and lox2272 sites to cause a flip in the construct, and the TATA-loxP concept. By inverting the orientation of the shRNA and EF1-alpha promoter, and placing them within a TATA-loxP-containing DIO cassette, I am able to express EGFP and the shRNA only after Cre recombination. Due to the size limitations of packaging into AAV, I used an H1 promoter, which is shorter than a U6 promoter. This did not affect expression of the shRNA, suggesting that the TATA-loxP is functional in both promoters, and it does not significantly affect the expression of shRNA in both promoters.

```
                                                  H1p
      MluI
1     ACGCGTCATA TTTGCATGTC GCTATGTGTT CTGGGAAATC ACCATAAACG
      TGCGCAGTAT AAACGTACAG CGATACACAA GACCCTTTAG TGGTATTTGC
                                          H1p
                                                TATAloxP
51    TGAAATCTAG ATAACTTCGT ATAGTATAAA TTATACGAAG TTATCACGGT
      ACTTTAGATC TATTGAAGCA TATCATATTT AATATGCTTC AATAGTGCCA
      H1p                                                NdeI
                                lox2272                          SalI
101   AATAACTTCG TATAGGATAC TTTATACGAA GTTATCATAT GGCTAGCGTC
      TTATTGAAGC ATATCCTATG AAATATGCTT CAATAGTATA CCGATCGCAG
                                                XhoI
      SalI                                      AvaI
151   GACCAAAAAC TCTTTACACA CAGTGAAGTT CTCGAGAACT TCACTGTGTG
      CTGGTTTTTG AGAAATGTGT GTCACTTCAA GAGCTCTTGA AGTGACACAC
                                   FosB shRNA
                 KpnI
201   TAAAGAGCCG GTACCGTGAT AACTTCGTAT AATTTATACT ATACGAAGTT
      ATTTCTCGGC CATGGCACTA TTGAAGCATA TTAAATATGA TATGCTTCAA
        FosB shRNA                          TATAloxP
            AgeI
251   ATCTAGACCG GTGTACCATA ACTTCGTATA AAGTATCCTA TACGAAGTTA
      TAGATCTGGC CACATGGTAT TGAAGCATAT TTCATAGGAT ATGCTTCAAT
      TATAloxP                              lox2272
301   T
      A
      lo
```

**Figure 25: Sequence of DIOR-shRNA cassette. The EF1-alpha promoter is inserted in the reverse orientation using restriction enzyme sites Sal1 and Nde1.**

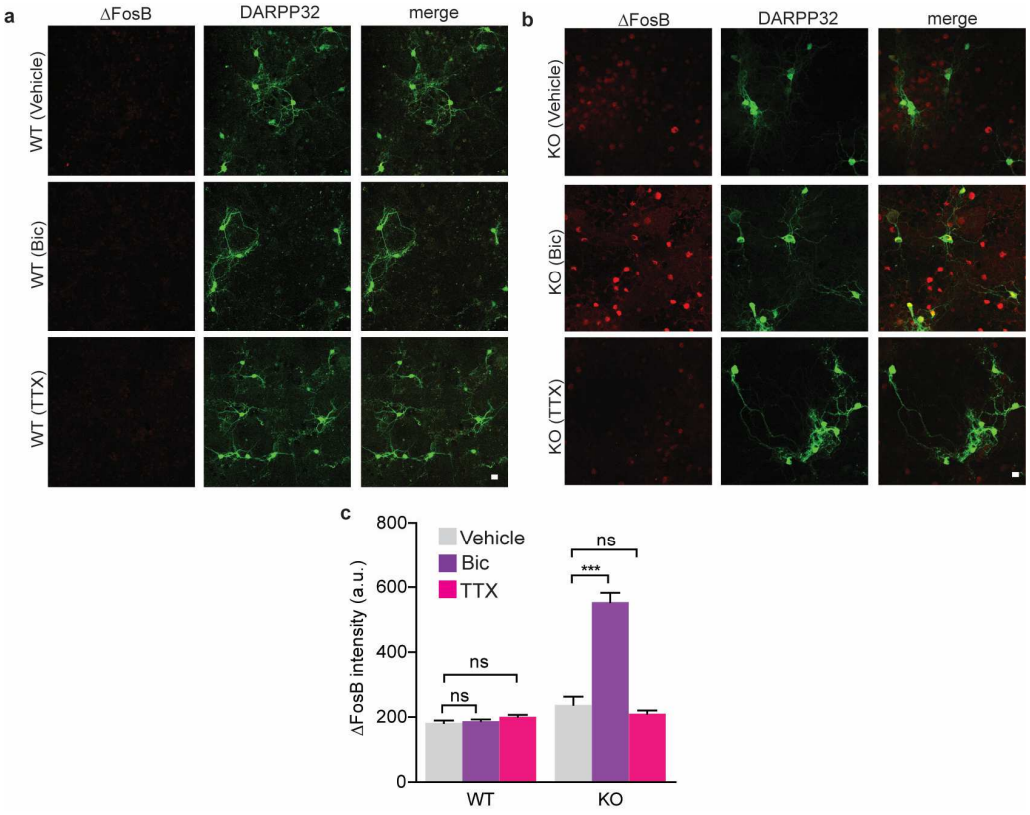


**Figure 26: Impaired homeostatic downscaling results in increased ΔFosB expression. a, Confocal images of wildtype (WT) medium spiny neurons (MSNs), labelled with DARPP32 (green), after 48 h of incubation with 40 μM bicuculline (Bic), 2 μM tetrodotoxin (TTX) or vehicle, starting at 10 days in vitro (DIV). No significant increase in ΔFosB (red) expression was observed after Bic or TTX incubation compared to vehicle (n=37 for vehicle, 25 for Bic, 77 for TTX). b, After 48 h of treatment with Bic, *Sapap3*$^{-/-}$ (KO) MSNs, labelled with DARPP32 (green), display higher levels of ΔFosB (red), compared to vehicle (n=74 for vehicle, 104 for Bic, 98 for TTX). c, Quantification of ΔFosB intensities showed significantly elevated ΔFosB expression in *Sapap3*$^{-/-}$ MSNs after 48 h of incubation with Bic. Scale bar: 10μm. ***P<0.001, ns: not significant, ANOVA with post-hoc Bonferroni test. Graphs show means±s.e.m.**

## *5.4 Preliminary homeostatic plasticity experiments*

Homeostatic plasticity, a form of homeostatic plasticity, involves the global and proportional scaling up of synapse strengths when the neuron has minimal activity, and the scaling down of synaptic weights when the neuron experiences enhanced firing rates. Homeostatic plasticity prevents runaway excitation of neural networks, so I conjectured that impaired homeostatic plasticity can exacerbate FosB accumulation. One way to induce homeostatic plasticity is to incubate neuronal cultures in bicuculline, a $GABA_A$ receptor antagonist, for 48 hours to induce scaling down of synapses. Another way is to incubate cultures in tetrodoxin (TTX) for 48 hours to induce scaling up of synapses. It has previously been shown in hippocampal cultures that knocking down GKAPs (of which Sapap3 is a member) results in impaired homeostatic scaling of synapses (Shin, 2012).

To test this hypothesis, I incubated cortico-striatal co-cultures from *Sapap3*-knockout and wildtype postnatal day 0 (P0) pups in bicuculline or TTX for 48 h starting at 10 days in vitro (DIV). Incubation of the cultures in bicuculline did not result in a significant elevation in FosB expression in wildtype MSNs (identified by DARPP32 staining), but significantly increased FosB expression in knockout MSNs. On the other hand, FosB expression was not significantly elevated after 48 hours of incubation with TTX, suggesting that the accumulation of FosB requires action potential firing. This was expected since transcription of immediate-early genes, such as FosB, is often driven by

calcium influx through voltage-gated calcium channels, which open during action potentials.

While this experiment suggests that knockout MSNs are more susceptible to FosB accumulation with increased excitatory input, confirming the role of Sapap3 in homeostatic scaling, it might not be instructive to the experience of MSNs *in vivo*. MSNs do not normally experience reduced inhibition or increased excitation for extended periods of time, and the environmental context where MSNs might experience enhanced excitatory input for days is uncertain.

This experiment will be relevant to behavior if we can link it with evidence obtained from chronic *in vivo* recordings. For instance, we can explore the circumstances where MSNs can experience enhanced synaptic input for extended periods of time, such as during recurrent stress from social defeat, chronic restraint stress or chronic unpredictable stress, environmental stimuli that are known to increase FosB expression (Perrotti, 2004). Other environmental factors that can be tested would be the repeated administration of drugs that enhance dopaminergic modulation such as cocaine, amphetamines or levodopa. These in vivo recordings will determine whether these environmental stimuli can lead to enhanced excitation of MSNs. We can then possibly correlate this observation with *in vitro* experiments showing that increased excitation or reduced inhibition can lead to FosB accumulation in *Sapap3*-knockout mice.

Moreover, if we pair the *in vivo* recordings with channelrhodopsin-based stimulation of thalamo-striatal and cortico-striatal axon terminals, we can even determine if there are stress-induced changes of specific inputs from the thalamus or cortex. A measure of the strength of the synaptic connection would be the slope of the channelrhodopsin-local field potential (ChR2-LFP) (Xiong, 2015). This would give us an idea of which synapses (thalamo-striatal or cortico-striatal) are affected by chronic stress or drugs of abuse, environmental factors that increase ΔFosB levels. For instance, one hypothesis suggests that in OCD, thalamo-striatal inputs are selectively potentiated after chronic stress, conveying signals that lead to greater attention and arousal to symptom-provoking stimuli (Kimura, 2004). Another hypothesis proposes that cortico-striatal connections, which encode reward paradigms, are selectively strengthened, leading to the perception that performing compulsive behaviors is more rewarding (Reynold, 2001). Of course, both connections may be strengthened in OCD. The use of channelrhodopsin for pathway-specific manipulations would enable the investigation of these two hypotheses.

# Chapter 6: Conclusion

OCD is a complex illness with varied degrees of severity, co-morbidities, clinical manifestations, genetic etiologies and treatment outcomes (Zhou, 2007; Mataix-Cols, 2004; Nestadt, 2010). The molecular and cellular mechanisms that underlie compulsions have been elusive. Yet discoveries using rodent models have provided insights to the cellular and molecular pathology of compulsive behavior.

The cortico-striatal-thalamo-striatal circuit controls many aspects of behavior, such as motor control, learning of action-outcome relationships, reinforcement learning and setting the level of motivation to seek appetitive stimuli. In particular, the orbitofrontal cortex and head of caudate – brain regions implicated in OCD – are involved in reinforcement learning, suggesting that aberrant reinforcement learning might underlie OCD. Our results suggest that accumulation of ΔFosB – a persistent transcription factor – in MSNs (particularly D1 MSNs) of this circuit underlies compulsive behavior. ΔFosB upregulates GluN2B, a NMDAR modulatory subunit that is involved in the aberrant formation of silent synapses, leading to the cortico-striatal synaptic defects and the imbalance of direct and indirect pathways implicated in OCD. In addition to elucidating the cellular mechanism of compulsive behaviors, I have dissected the cell type responsible for compulsive behavior, and identified a novel drug target for compulsive behavior, the GluN2B NMDAR modulatory subunit.

Imaging studies in patients with obsessive-compulsive disorder (OCD) have observed divergent striatal responses to symptom-provoking and reward-predicting stimuli. Functional magnetic resonance imaging (fMRI) studies on OCD patients have identified increased striatal activity at baseline and during provocation studies (Menzies, 2008), but blunted responses during exposure to reward cues in the reward anticipation task (Figee, 2013). Studies using rodent models are similar. Striatal *in vivo* recordings in the *Sapap3*-null (*Sapap3*$^{-/-}$) OCD mouse model revealed increased medium spiny neuron (MSN) firing rates at baseline and during compulsive grooming (Burguiere, 2013). Yet $\alpha$-amino-3-hydroxy-5-methyl-4-isoxazolepropionic acid receptor (AMPAR)-mediated cortico-striatal field potentials and miniature excitatory post-synaptic currents (mEPSCs) are diminished in rodent models of OCD (Shmelkov, 2010; Welch, 2007; Wan Y., 2011). Sapap3 is necessary for stabilization of *N*-methyl-D-aspartate receptors (NMDARs) at cortico-striatal synapses, but not at thalamo-striatal synapses (Wan, 2014). "Bottom-up" thalamo-striatal connections encode arousal and attention to salient external events (Kimura, 2004), whereas "top-down" cortico-striatal synapses encode reward contingencies (Xiong, 2015; Reynold, 2001). Thus, stronger thalamo-striatal connections and weaker cortico-striatal connections might result in the saliency of stimuli overshadowing its actual reward value, potentially fueling compulsive behaviors.

Striatal expression of the transcription factor ΔFosB exerts striking effects on motivation and movement. Abnormally high levels in D1 dopamine receptor-expressing medium spiny neurons (D1 MSNs) results in addiction (Nestler, 2008) and dyskinesias (Anderson, 1999), whereas relatively low levels causes clinical depression (Vialou, 2010) and catatonia (Bonito-Oliva, 2011). Moreover, thalamo-striatal afferent fibers preferentially innervate D1 MSNs (Sidibe, 1996), and ΔFosB expression can be induced in D1 MSNs by salient stimuli like chronic stress (Perrotti, 2004), drugs of abuse (Kelz, 1999) and levodopa (Bonito-Oliva, 2011). Unlike the other Fos isoforms that are expressed transiently and display tolerance, ΔFosB persists for at least several weeks, even enduring for months, in neurons after its initial induction (Nestler, 1999). Interestingly, ΔFosB preferentially promotes GluN2B expression in D1 MSNs (Grueter, 2013). GluN2B, a modulatory subunit of NMDARs, promotes long-term potentiation (LTP) at functional synapses (such as thalamo-striatal synapses in *Sapap3*$^{-/-}$ mice) due to its slow channel kinetics (Foster, 2010; Tang, 1999). Conversely, at immature synapses (such as cortico-striatal synapses in *Sapap3*$^{-/-}$ mice), GluN2B inhibits the recruitment of AMPARs (Gray, 2011; Huang, 2009; Hall, 2007). Taken together, these findings suggest that abnormal ΔFosB levels in D1 MSNs underlie pathological behaviors, and dovetail with our results, which show that ΔFosB elevation in D1 MSNs cause compulsive behaviors.

However, the findings from rodent models have not been extended to studies involving human OCD patients. It is unclear if postmortem brain tissue from the caudate of patients with OCD have increased ΔFosB levels, or if these patients will respond positively to GluN2B antagonists. Finally, repetitive behaviors are observed in several neuropsychiatric disorders, such as OCD, trichotillomania, Tourette syndrome, and autism (Allen, 2003). If the molecular mechanism mediating repetitive behavior is commonly shared among these various obsessive-compulsive spectrum disorders, this concept could inform the classification and treatment of these myriad neuropsychiatric disorders. Likewise, high ΔFosB levels in D1 MSNs are associated with levodopa-induced dyskinesia and drug addiction, whereas relatively lower levels are associated with haloperidol-induced dystonia and clinical depression. Therefore, our findings may also be relevant to other disorders that are caused by aberrant ΔFosB levels.

# Bibliography

**Abelson, JF, et al. 2005.** Sequence variants in SLITRK1 are associated with Tourette's Syndrome. *Science.* 2005, Vol. 310, 5746, pp. 317-320.

**Aboujaoude, E., Barry, J.J. & Gamel, N. 2009.** Memantine augmentation in treatment-resistent obsessive-compulsive disorder: an open-label trial. *J. Clin. Psychopharmacol.* 2009, Vol. 29, 1, pp. 51-55.

**Ahmari, S.E., Spellman, T., Douglass, N.L., Kheirbek, M.A., Simpson, H.B., Deisseroth, K., Gordon, J.A. & Hen, R. 2013.** Repeated cortico-striatal stimulation generates persistent OCD-like behavior. *Science.* 2013, Vol. 340, pp. 1234-8.

**Allen, A., King, A. & Hollander, E. 2003.** Obsessive compulsive spectrum disorders. *Dialogues Clin. Neurosci.* 2003, Vol. 5, pp. 259-271.

**Alonso, P., Gratacos, M., Segalas, C., Georgia, E., Real, E., Bayes, M., Labad, J., Lopez-Sola, C., Estivill, X. & Menchon, J.M. 2012.** Association of NMDA glutamate receptor gene GRIN2B with obsessive-compulsive disorder. *J. Psychiatry Neurosci.* 4, 2012, Vol. 37, pp. 273-281.

**American Psychiatric Association. 2000.** *Diagnostic and Statistical Manual of Mental Disorders, DSM-IV-TR, 4th ed.* Arlington : Author, 2000.

**Anderson, M., et al. 1999.** Striatal FosB expression is causally linked with L-DOPA-induced involuntary movements and the associated upregulation of striatal pro-dynorphin mRNA in a rat model of Parkinson's disease. *Neurobiol Dis.* 1999, Vol. 6, pp. 461-474.

**Arnold, P.D., et al. 2004.** Association of a glutamate (NMDA) subunit receptor gene (GRIN2B) with obsessive-compulsive disorder: a preliminary study. *Psychopharmacology.* 174, 2004, Vol. 4, pp. 530-8.

**—. 2009.** Glutamate receptor gene (GRIN2B) associated with reduced anterior cingulate glutaminergic concentration in pediatric obsessive-compulsive disorder. *Psychiatry Res.* 2009, Vol. 172, 2, pp. 136-139.

**—. 2006.** Glutamate transporter gene SLC1A1 associated with obsessive-compulsive disorder. *Arch Gen Psychiatry.* 2006, Vol. 63, 7, pp. 769-76.

**Ashby, M.C. & Isaac, J.T. 2011.** Maturation of a recurrent excitatory neocortical circuit by experience-dependent unsilenceing of newly formed dendritic spines. *Neuron.* 2011, Vol. 70, pp. 510-521.

**Berntson, G.G, et al. 2007.** Amygdala contribution to selective dimensions of emotion. *Soc Cogn Affect Neurosci.* 2007, Vol. 2, 2, pp. 123-129.

**Berton, O, et al. 2009.** Striatal overexpression of deltaJunD resets L-DOPA-induced dyskinesia in a primate model of Parkinson's disease. *Biol Psychiatry.* 66, 2009, pp. 554-561.

**Bienvenu, O.J., et al. 2009.** Sapap3 and pathological grooming in humans: Results from the OCD collaborative genetics study. *Am J Med Genet B Neuropsychiatr Genet.* 2009, Vol. 150B, 5, pp. 170-120.

**—. 2000.** The relationship of obsessive–compulsive disorder to possible spectrum disorders: results from a family study. *Biol Psychiatry.* 2000, Vol. 48, 4, pp. 287-293.

**Bloch, M.H., et al. 2012.** Effects of ketamine in treatment-refractory obsessive-compulsie disorder. *Biol. Psychiatry.* 2012, Vol. 72, pp. 964-970.

**Boardman, L., van der Merwe, L., Lochner, C., Kinnear, C.J., Seedat, S., Stein, D.J., Moolman-Smook, J.C. & Hemmings, S.M.J. 2011.** Investigating SAPAP3 variants in the etiology of obsessive-compulsive disorder and trichotillomania in the South African white population. *Compr. Psychiatry.* 2011, Vol. 52, 2, pp. 181-187.

**Bonito-Oliva, A, Feyder, M. & Fisone, G. 2011.** Deciphering the actions of antiparkinsonian and antipsychotic drugs on cAMP/DARRP-32 signalling. *Front. Neuroanat.* 2011, Vol. 5, 38, pp. 1-9.

**Brigman, J.L., et al. 2013.** GluN2B in corticostriatal circuits governs choice learning and choice shifting. *Nat Neurosci.* doi:10.1038/nn.3457, 2013.

**Brown J.R., Ye H., Bronson R.T., Dikkes P. & Greenberg M.E. 1996.** A defect in nurturing in mice lacking the immediate early gene fosB. *Cell.* 1996, Vol. 86, 2, pp. 297-309.

**Brown, T.E., et al. 2011.** A Silent Synapse-based Mechanism for Cocaine-induced Locomotor Sensitization. *J Neurosci.* 2011, Vol. 31, 22, pp. 8163-8174.

**Burguiere, E., Monteiro, P., Feng, G. & Graybiel, A.M. 2013.** Optogenetic stimulation of lateral orbitofrontal-striatal pathway suppresses compulsive behaviors. *Science.* 2013, Vol. 340, pp. 1243-1246.

**Burrone, J. & Murthy, V.N. 2003.** Synaptic gain control and homeostasis. *Curr. Opin. Neurobiol.* 2003, Vol. 13, pp. 560-567.

**Butelman, E.R., Yuferov, V. & Kreek, M.J. 2012.** K-opioid receptor/dynorphin system: genetic and pharmacotherapeutic implications for addiction. *Trends Neurosci.* 2012, Vol. 35, 10, pp. 587-596.

**Cao, X, et al. 2010.** Striatal overexpression of deltaFosB reproduces chronic L-DOPA-induced involuntary movements. *J Neurosci.* 2010, Vol. 30, pp. 7335-7343.

**Capecchi, M.R. 1997.** Hox genes and mammalian development. *Cold Spring Harb Symp Quant Biol.* 1997, Vol. 67, pp. 273-281.

**Carey, G, Gottesman II. 1981.** Twin and family studies of anxiety, phobic and obsessive disorders. [book auth.] DF & Rabkin, JG. Klein. *Anxiety: New research and changing concepts.* 1981, pp. 117-136.

**Chen, B.S., et al. 2012.** SAP102 mediates synaptic clearance of NMDA receptors. *Cell Rep.* 2012, Vol. 2, pp. 1120-1128.

**Chen, L., Bohanick, J.D., Nishihara, M., Seamans, J.K. and Yang, C.R. 2007.** Dopamine 1/5 receptor-mediated potentiation of intrinsic excitability of rat prefrontal cortical neurons: calcium-dependent intracellular signalling. 2007, Vol. 97, pp. 2448-2464.

**Chen, S.K., Tvrdik, P., Peden, E., Cho, S., Wu, S., Spangrude, G. & Capecchi, M.R. 2010.** Hematopoietic origin of pathological grooming in Hoxb8 mutant mice. *Cell.* 2010, Vol. 141, pp. 775-785.

**Choe, C. & Ehrlich, B.E. 2006.** The inositol 1,4,5-triphosphate receptor (IP3R) and its regulators: sometimes good and sometime bad teamwork. *Sci STKE.* 2006, Vol. 363, p. re15.

**Chuhma N., Tanaka K.F., Hen R. & Rayport S. 2011.** Functional connectome of the striatal medium spiny neuron. *J Neurosci.* 2011, Vol. 31, 4, pp. 1138-1192.

**Clarke, L.E. & Barres, B.A. 2013.** Emerging roles of astrocytes in neural circuit development. *Nat Rev Neurosci.* 2013, Vol. 14, pp. 311-21.

**Close, J., et al. 2012.** Stab1 is an activity-modulated transcription factor required for terminal diffentiation and connectivity of MGE-derived interneurons. *J. Neurosci.* 2012, Vol. 32, 49, pp. 17690-17705.

**Cohen, S. et al. 2011.** Genome-wide activity-dependant MeCP2 phosphorylation regulates nervous system development and cognitive function. *Neuron.* 2011, Vol. 72, pp. 72-85.

**Crum, RM & Anthony, JC. 1993.** Cocaine use and other suspected risk factors for obsessive-compulsive disorder: a prospective study with data from the Epidemiologic Catchment Area surveys. *Drug Alcohol Depend.* 1993, Vol. 31, 3, pp. 281-95.

**Cui, G, et al. 2013.** Concurrent activation of striatal direct and indirect pathways during action initiation. *Nature.* 2013, Vol. 494, pp. 238-242.

**Davis, G.W. 2013.** Homeostatic signaling and the stabilization of neural function. *Neuron.* 2013, Vol. 80, 3, pp. 718-728.

**Denys, D., Mantione, M., Figee, M., van den Munckhof, P., Koerselman, F., Westenberg, H., et al. 2010.** Deep brain stimulation of the nucleus accumbens for treatment-refractory obsessive-compulsive disorder. *Arch. Gen. Psychiatry.* 2010, Vol. 67, 10, pp. 1061-1068.

**Dietrich, M.O., et al. 2015.** Hypothalamic Agrp neurons drive stereotypic behaviors beyond feeding. *Cell.* 2015, Vol. 160, 6, pp. 1222-1232.

**Doucet, JP et al. 1996.** Chronic alterations in dopaminergic neurotransmission produce a persistent elevation of deltaFosB-like protein(s) in both the rodent and primate striatum. *Eur J Neurosci.* 1996, Vol. 8, 2, pp. 365-81.

**Elias, G.M., Elias, L.A., Apostolides, P.F., Kriegstein, A.R., & Nicoll, R.A. 2008.** Differential trafficking of AMPA and NMDA receptors by SAP102 and PSD-95 underlies synaptic development. *Proc Natl Acad Sci USA.* 2008, Vol. 105, pp. 20953-8.

**Everitt, B.J. & Robbins, T.W. 2005.** Neural systems of reinforcement for drug addiction: from actions to habits to compulsion. *Nature Neurosci.* 2005, Vol. 8, pp. 1481-1489.

**Figee, M., et al. 2013.** Deep brain stimulation restores frontostriatal network activity in obsessive-compulsive disorder. *Nat Neurosci.* 2013, Vol. 16, pp. 386-7.

**Foster, K.A., McLaughlin, N., Edbauer, D., Phillips, M., Bolton, A., Constantine-Paton, M. & Sheng, M. 2010.** Distinct roles of NR2A and NR2B cytoplasmic tails in long-term potentiation. *J. Neurosci.* 2010, Vol. 30, 7, pp. 2676-85.

**Fukunaga, K., Goto S. and Miyamoto E. 1988.** Immunohistochemical localization of calcium/calmodulin-dependent protein kinase II in rat brain and various tissues. 1988 *йил*, pp. 1070-1078.

**Gershuny, B.S., Baer, L., Parker, H., Gentes, E.L., Infield, A.L. & Jenike, M.A. 2008.** Trauma and post-traumatic stress disorder in treatment-resistant obsessive-compulsive disorder. *Depress. Anxiety.* 2008, Vol. 25, 1, pp. 69-71.

**Glimcher, PW. 2011.** Understanding dopamine and reinforcement learning: The dopamine reward prediction error hypothesis. *PNAS.* 2011, Vol. 108, pp. 15647-54.

**Gong, S., et al. 2003.** A gene expression atlas of the central nervous system based on bacterial artificial chromosomes. *Nature.* 2003, Vol. 425, pp. 917-925.

**Gorski, J.A., Talley, T., Qiu, M., Rubenstein, J.L.R. & Jones, K.R. 2002.** Cortical excitatory neurons and glia, but not GABAergic neurons, are produced in Emx1-expressing lineage. *J. Neurosci.* 2002, Vol. 22, 15, pp. 6309-6314.

**Grados, MA. 2010.** The genetics of obsessive-compulsive disorder and Tourette syndrome: an epidemiological and pathway-based approach for gene discovery. *J Am Acad Child Adolesc Psychiatry.* 2010, Vol. 49, pp. 810-819.

**Granger, AJ, et al. 2013.** LTP requires a reserve pool of glutamate receptors independent of subunit type. *Nature.* 2013, Vol. 493, pp. 495-500.

**Gray, J.A., Shi, Y., Usui, H., During, M.J., Sakimura, K. & Nicoll, R.A. 2011.** Distinct modes of AMPA receptor suppression at developing synapses by GluN2A and GluN2B: single-cell NMDA receptor subunit deletion in vivo. *Neuron.* 2011, Vol. 71, pp. 1085-1101.

**Graybiel, A. M., and Rauch S. L. 2000.** Toward a neurobiology of obsessive-compulsive disorder. *Neuron.* 2000, Vol. 28, pp. 343-347.

**Greenburg, B.D., Malone, D.A., Friehs, G.M., Kubu, C.S., Malloy, P.F., Salloway, S.P., Goodman, W.K. & Rasmussen, S.A. 2006.** Three-year outcomes in deep brain stimulation for highly resistant obsessive-compulsive disorder. *Neuropsychopharmacology.* 2006, Vol. 31, pp. 2384-2393.

**Greer, J.M. & Capecchi, M.R. 2002.** Hoxb8 is required for normal grooming behavior in mice. *Neuron.* 2002, Vol. 33, 1, pp. 23-34.

**Grueter, B.A., Robison, A.J., Neve, R.L., Nestler, E.J. & Malenka, R.C. 2013.** ΔFosB differentially modulates nucleus accumbens direct and indirect pathway functions. *Proc. Natl. Acad. Sci. USA.* 2013, Vol. 10, 5, pp. 1923-1928.

**Gubelmann, C., Gattiker, A., Massouras, A., Hens, K., David, F., Decouttere, F., Rougemont, J. & Deplancke, B. 2011.** GETPrime: A gene- or transcript-specific primer database for quantitative real-time PCR. *Database.* 2011, Vol. 2011, p. bar040.

**Haber S.N., Kunishio K., Mizobuchi M. & Lynd-Balta E. 1995.** The orbital and medial prefrontal circuit through the primate basal ganglia. *J Neurosci.* 1995, Vol. 15, pp. 1451-1467.

**Hall, B.J., Ripley, B. & Ghosh, A. 2007.** NR2B signaling regulates the development of synaptic AMPA receptor current. *J. Neurosci.* 2007, Vol. 27, pp. 13446-56.

**Hanse, E., Seth, H., & Riebe, I. 2013.** AMPA-silent synapses in brain development and pathology. *Nat Rev Neurosci.* 2013, Vol. 14, pp. 839-850.

**Hare, T.A., O'Doherty, J., Camerer, C.F., Schultz, W. & Rangel, A. 2008.** Dissociating the Role of the Orbitofrontal Cortex and the Striatum in the Computation of Goal Values and Prediction Errors. *J Neurosci.* 2008, Vol. 28, 22, pp. 5623-5630.

**Harrison, B.J., et al. 2009.** Altered corticostriatal functional connectivity in obsessive-compulsive disorder. *Arch Gen Psychiatry.* 2009, Vol. 66, 11, pp. 1189-1200.

**Hasler, G. et al. 2007.** Familiality of Factor Analysis-Derived YBOCS Dimensions in OCD-Affected Sibling Pairs from the OCD Collaborative Genetics Study. *Biol Psychiatry.* 5, 2007, Vol. 61, pp. 617-625.

**Hikida, T., Kimura, K., Wada, N., Funabiki, K. & Nakanishi, S. 2010.** Distinct roles for striatal transmission in direct and indirect striatal pathways to reward and aversive behaviors. *Neuron.* 2010, Vol. 66, pp. 896-907.

**Hiroi, N., et al. 1998.** Essential role of the fosB gene in molecular, cellular, and behavioral actions of chronic electroconvulsive seizures. *J Neurosci.* 1998, Vol. 18, 17, pp. 8952-8962.

**Holstege, J.C., et al. 2008.** Loss of Hoxb8 alters spinal dorsal laminae and sensory responses in mice. *Proc Natl Acad Sci USA.* 2008, Vol. 105, pp. 6338-6343.

**Huang, Y.H., et al. 2009.** In Vivo Cocaine Experience Generates Silent Synapses. *Neuron.* 2009, Vol. 63, pp. 40-47.

**Jennings, J. et al. 2013.** Distinct extended amygdala circuits for divergent motivational states. *Nature.* 2013, Vol. 10, p. 12041.

**Jessberger, S., et al. 2009.** Making a neuron: Cdk5 in embryonic and adult neurogenesis. *Trends Neurosci.* 2009, Vol. 32, 11, pp. 575-582.

**Jia, Z., et al. 1996.** Enhanced LTP in mice deficient in the AMPA receptor GluR2. *Neuron.* 1996, Vol. 17, 5, pp. 945-956.

**Jones, E.G., Huntley, G.W. and Benson, D.L. 1994.** Alpha calcium/calmodulin protein kinase II selectively expressed in subpopulations of neurons in the monkey sensory-motor cortex: comparison with GAD67 expression. 1994 *йил*, pp. 611-629.

**Katayama, K., et al. 2010.** Slitrk1-deficient mice display elevated anxiety-like behavior and noradrenergic abnormalities. *Mol Psychiatry.* 2010, Vol. 15, pp. 177-184.

**Keck, T., et al. 2013.** Synaptic scaling and homeostatic plastitcity in the mouse visual cortex in vivo. *Neuron.* 2013, Vol. 80, 2, pp. 327-334.

**Kelz, M.B., Chen, J., Carlezon, W.A., et al. 1999.** Expression of the transcription factor deltaFosB in the brain controls sensitivity to cocaine. *Nature.* 1999, Vol. 410, pp. 272-276.

**Kerchner, G.A. & Nicoll, R.A. 2008.** Silent synapses and the emergence of a postsynaptic mechanism for LTP. *Nat. Rev. Neurosci.* 2008, Vol. 9, 11, p. 813.

**Kessler, R.C., Chiu, W.T., Demler, O. & Walters, E.E. 2005.** Prevalence, severity, and comorbidity of 12-Month DSM-IV disorders in the National Comorbidity Survey Replication. *Arch. Gen. Psychiatry.* 2005, Vol. 62, pp. 617-627.

**Kimura, M., Minamimoto, T., Mastsumoto, M. & Hori, Y. 2004.** Monitoring and switching of cortico-basal ganglia loop functions by the thalamo-striatal system. *Neurosci Res.* 2004, Vol. 48, pp. 355-360.

**Kozorovitskiy, Y., Saunder, A., Johnson, C.A., Lowello, B.B. & Sabatini, B.L. 2012.** Recurrent network activity drives striatal synaptogenesis. *Nature.* 2012, Vol. 485, pp. 646-650.

**Kreitzer, A.C. 2009.** Physiology and pharmacology of striatal neurons. *Annu. Rev. Neurosci.* 2009, Vol. 32, pp. 127-147.

**Lai, K-O. & Yip, N. 2009.** Recent advances in understanding the roles of Cdk5 in synaptic plasticity. *BBA.* 2009, Vol. 1792, 8, pp. 741-745.

**Lee, M-C., Yasuda, R. & Ehlers, M.D. 2010.** Metaplasticity at single glutamatergic synapses. *Neuron.* 2010, Vol. 66, pp. 859-870.

**Lively, S. & Brown, I.R. 2008.** The extracellular matrix protein SC1/hevin localizes to excitatory synapses following status epilepticus in the rat lithium-pilocarpine seizure model. *J Neurosci Res.* 2008, Vol. 86, pp. 2895-2905.

**Lochner, C., et al. 2002.** Childhood trauma in obsessive-compulsive disorder, trichotillomania, and controls. *Depress Anxiety.* 2002, Vol. 15, pp. 66-68.

**Logothetis, N.K., Pauls, J., Augath, M., Trinath, T. and Oeltermann, A. 2001.** Neurophysiological investigation of the basis of the fMRI signal. *Nature.* 2001, Vol. 412, pp. 150-157.

**Lu X.Y., Ghasemzadeh M.B. & Kalivas P.W. 1998.** Expression of D1 receptor, D2 receptor, substance P and enkephalin messenger RNAs in the neurons projecting from the nucleus accumbens. *Neuroscience.* 1998, Vol. 82, 3, pp. 767-780.

**Mataix-Cols, D., et al. 2004.** Distinct neural correlates of washing, checking, and hoarding symptom dimensions in obsessive-compulsive disorder. *Arch Gen Psychiatry.* 2004, Vol. 61, 6, pp. 564-576.

**Mattheisen, M., et al. 2014.** Genome-wide association study in obssesive-compulsive disorder: results from the OCGAS. *Mol. Psychiatry.* 2014, pp. 1-8.

**McDonald, A.J. 1991.** Topographical organization of amygdaloid projections to the caudoputamen, nucleus accumbens and related striatal-like areas of the rat brain. *Neuroscience.* 1991, Vol. 44, 1, pp. 15-33.

**McDougle, CJ, Goodman, WK, Leckman, JF, Lee, NC, Heninger, GR & Price, LH. 1994.** Haloperidol addition in fluvoxamine-refractory obsessive-compulsive disorder.

A double-blind, placebo-controlled study in patients with and without tics. *Arch Gen Psychiatry.* 1994, Vol. 51, 4, pp. 302-8.

**Menzies, L., Chamberlain, S.R., Laird, A.R., Thelen, S.M., Sakakian, B.J. & Bullmore, E.T. 2008.** Integrating evidence from neuroimaging and neuropsychological studies of obsessive-compulsive disorder: The orbito-frontal striatal model revisited. *Neurosci Neurobehav Rev.* 2008, Vol. 32, pp. 525-549.

**Monyer, H., et al. 1994.** Developmental and regional expression in the rat brain and functional properties of four NMDA receptors. *Neuron.* 1994, Vol. 12, pp. 529-540.

**Nacasch, N., Fostick, L. & Zohar, J. 2011.** High prevalence of obsessive-compulsive disorder among post-traumatic stress disorder patients. *Eur. Neuropsychopharm.* 2011, Vol. 21, 12, pp. 876-879.

**Nakabeppu, Y & Nathans, D. 1991.** A naturally occurring truncated form of FosB that inhibits Fos/Jun transcriptional activity. *Cell.* 1991, Vol. 65, 4, pp. 751-759.

**Nestadt, G, Grados, M & Samuels, JF. 2010.** Genetics of OCD. *Psychiatr Clin North Am.* 2010, Vol. 33, 1, pp. 141-158.

**Nestadt, G., et al. 2000.** A Family Study of Obsessive-compulsive Disorder. *Arch Gen Psychiatry.* 2000, Vol. 57, pp. 358-363.

**Nestler, E.J. 2008.** Transcriptional mechanisms of addiction: role of ΔFosB. *Philos. Trans. R. Soc. Lond. B Biol. Sci.* 2008, Vol. 363, 1507, pp. 3245-3255.

**Nestler, E.J., Barret, M. & Self, D.W. 2001.** ΔFosB: A sustained molecular switch for addiction. *PNAS.* 2001, Vol. 98, 20, pp. 11042-46.

**Nestler, E.J., Kelz, M.B. & Chen J. 1999.** ΔFosB: a molecular mediator of long-term neural and behavioral plasticity. *Brain Res.* 1999, Vol. 835, pp. 10-17.

**Ochiishi T., Terashima, T. and Yamaguchi, T. 1994.** Specific distribution of calcium/calmodulin dependent kinase II alpha and beta isoforms in some structures in the forebrain. 1994 *йил*, pp. 179-193.

**Oh, S.W., et al. 2014.** A mesoscale connectome of the mouse brain. *Nature.* 2014, Vol. 508, pp. 207-14.

**O'Neill, LAJ & Kaltschmidt, C. 1997.** NF-kB: a crucial transcription factor for glial and neuronal cell function. *Trends Neurosci.* 1997, Vol. 20, 6, pp. 252-258.

**Ouimet, C.C., McGuiness T.L. and Greengard, P. 1984.** Immunocytochemical localization of calcium/calmodulin-dependent protein kinase II in rat brain. 1984 *йил*, pp. 81:5604-5608.

**Pascual, O., et al. 2012.** Microglia activation triggers astrocyte-mediated modulation of excitatory neurotransmission. *PNAS.* 2012, Vol. 109, 4, pp. E197-E205.

**Passafaro, M., et al. 2003.** Induction of dendritic spines by an extracellular domain of AMPA receptor subunit GluR2. *Nature.* 2003, Vol. 424, pp. 677-681.

**Pauls, D.L., Abramovich, A., Rauch, S.L. & Geller, D.A. 2014.** Obsessive-compulsive disorder: an integrative genetic and neurobiological perspective. *Nat. Rev. Neurosci.* 2014, Vol. 15, pp. 410-424.

**Perrotti, L.I., Hadeishi, Y., Ulery, P.G., Barrot, M., Monteggia, L., Duman, R.S. & Nestler, E.J. 2004.** Induction of ΔFosB in reward-related brain structures after chronic stress. *J. Neurosci.* 2004, Vol. 24, 47, pp. 10594-10602.

**Peters, J., et al. 2009.** Extinction circuits for fear and addiction overlap in the prefrontal cortex. *Learn Mem.* 2009, Vol. 16, pp. 279-288.

**Pittenger, C., Bloch, M.H., & Williams, K. 2011.** Glutamate abnormalities in obsessive compulsive disorder: Neurobiology, pathophysiology and treatment. *Pharmacol Therapeut.* 2011, Vol. 132, pp. 314-332.

**Plattner, F., et al. 2014.** Memory enhancement by targeting Cdk5 regulation of NR2B. *Cell.* 2014, Vol. 81, pp. 1070-83.

**Proenca, C.C., et al. 2011.** Slitrks as emerging candidate genes involved in neuropsychiatric disorders. *Trends Neurosci.* 2011, Vol. 34, 3, pp. 143-153.

**Qian, C., et al. 2012.** Imaging Neural Activity Using Thy1-GCaMP Transgenic Mice. 2012, Vol. 76, 2, pp. 297-308.

**Qiang, M & Ticku, M.K. 2005.** Role of AP-1 in ethanol-induced N-methyl-D-aspartate receptor 2B subunit gene up-regulation in mouse cortical neurons. *J Neurochem.* 2005, Vol. 95, 5, pp. 1332-41.

**Ragozzino, M.E. 2007.** The contribution of the medial prefrontal cortex, orbitofrontal cortex, and dorsomedial striatum to behavioral flexibility. *Ann. N. Y. Acad. Sci.* 2007, Vol. 1121, pp. 355-75.

**Ramocki, M.B. & Zoghbi, H.Y. 2008.** Failure of neuronal homeostasis results in common neuropsychiatric phenotypes. *Nature.* 2008, Vol. 455, pp. 912-918.

**Reynold, J.N.J., Hyland, B.I. & Wickens, J.R. 2001.** A cellular mechanism of reward-related learning. *Nature.* Vol. 413, pp. 67-70.

**Richard, J.M & Berridge, K.C. 2011.** Nucleus Accumbens Dopamine/Glutamate Interaction Switches Modes to Generate Desire versus Dread: D1 Alone for Appetitive Eating But D1 and D2 Together for Fear. *J Neurosci.* 2011, Vol. 31, 36, pp. 12866-12879.

**Rodriguez, C.I., Kegeles, L.S., Flood, P. & Simpson, H.B. 2011.** Rapid resolution of obsessions after infusion of intravenous ketamine in patient with treatment-resistant obsessive-compusive disorder. *J. Clin. Psychiatry.* 2011, Vol. 72, 4, pp. 567-569.

**Romorini, S., et al. 2004.** A functional role of postsynaptic density-95-guanylate kinase-associated protein complex in regulating Shank assembly and stability to synapses. *J. Neurosci.* 2004, Vol. 24, pp. 9391-9404.

**Sakai Y., Narumoto J., Nishida S., Nakamae T., Yamada K., Nishimura T. & Fukui K. 2011.** Corticostriatal functional connectivity in non-medicated patients with obsessive-compulsive disorder. *Eur Psychiatry.* 2011, Vol. 26, 7, pp. 463-469.

**Samuels, JF, et al. 2006.** The OCD Collaborative Genetics Study: Methods and Sample Description. *Am J Med Genet B Neuropsychiatr Genet.* 2006, Vol. 141B, 3, pp. 201-207.

**Sans, N., et al. 2000.** A developmental change in NMDA receptor associated proteins at hippocampal synapses. *J. Neurosci.* 2000, Vol. 20, 3, pp. 1260-1271.

**Schiff, N.D. 2008.** Regulation and neurological disorders of consciousness. *Ann N Y Acad Sci.* 2008, Vol. 1129, pp. 105-118.

**Schnutgen, F., Doerflinger, N., Calleja, C., Wendling, O., Chambon, P. & Ghyselinck, N.B. 2003.** A directional strategy for monitoring Cre-mediated recombination at the cellular level in the mouse. *Nat. Biotech.* 2003, Vol. 21, pp. 562-565.

**Scimemi, A., et al. 2009.** Neuronal transporters regulate glutamate clearance, NMDA receptor activation and synaptic plasticity in the hippocampus. *J Neurosci.* 2009, Vol. 29, 46, pp. 14581-14595.

**Sheng, M. & Hoogenraad, C.C. 2007.** The postsynaptic architure of excitatory synapses: a more quantitative view. *Annu. Rev. Biochem.* 2007, Vol. 76, pp. 823-847.

**Shin, S.M., Zhang, N., Hansen, J., Verges, N.Z., Pak. D.T.S., Sheng, M. & Lee, S.H. 2012.** GKAP orchestrates activity-dependent postsynaptic protein remodeling and homeostatic scaling. *Nat. Neuroscience.* 2012, Vol. 15, 12, pp. 1655-1666.

**Shiromani P.J., Basheer R., Thakkar J., Wagner D., Greco M.A. & Charness M.E. 2000.** Sleep and wakefulness in c-fos and fos B gene knockout mice. *Brain Res Mol Brain Res.* 2000, Vol. 80, 1, pp. 75-87.

**Shmelkov, S.V., et al. 2010.** Slitrk5 deficiency impairs corticostriatal circuitry and leads to obsessive-compulsive-like behaviors in mice. *Nat. Med.* 2010, Vol. 15, 5, pp. 598-602.

**Shuen, J., Chen, M., Gloss, B. & Calakos, N. 2008.** Drd1a-tdTomato BAC transgenic mice for simultaneous visualization of medium spiny neurons in the direct and indirect pathways of the basal ganglia. *J. Neurosci.* 28, 2008, Vol. 11, pp. 2681-2685.

**Sidibe, M. & Smith Y. 1996.** Differential synaptic innervation of striatofugal neurones projecting to the internal or external segments of the globus pallidus by thalamic afferents in the squirrel monkey. *J. Comp. Neurol.* 1996, Vol. 365, pp. 445-465.

**Simms, B.A. & Zamponi, G.W. 2014.** Neuronal voltage-gated calcium channels: stucture, function and dysfunction. *Cell.* 2014, Vol. 82, 1, pp. 24-45.

**Stellwagen, D. & Malenka, R.C. 2006.** Synaptic scaling mediated by glial TNF-alpha. *Nature.* 2006, Vol. 440, pp. 1054-1059.

**Steward, S.E., et al. 2013.** Genome-wide association study of obsessive-compulsive disorder. *Mol. Psychiatry.* 2013, Vol. 18, pp. 709-805.

**Stewart, S.E., Jenike, E.A., Hezel, D.M., Stack, D.E., Dodman, N.H., Shuster, L. & Jenike, M.A. 2010.** A single-blinded case-control study of memantine in severe obsessive-compulsive disorder. *J. Clin. Psychopharmacol.* 30, 2010, Vol. 1, pp. 34-39.

**Stuber, G.D., et al. 2011.** Excitatory transmission from the amygdala to nucleus accumbens facilitates reward learning. *Nature.* 2011, Vol. 475, pp. 377-380.

**Takahashi, H., et al. 2012.** Selective control of inhibitory synapse development by Slitrk5-PTPdelta transynaptic interaction. *Nat. Neuroscience.* 2012, Vol. 15, 3, pp. 389-398.

**Tang, Y.P., et al. 1999.** Genetic enhancement of learning and memory in mice. *Nature.* 1999, Vol. 401, pp. 63-69.

**Taylor, C.W & Tovey, S.C. 2010.** IP3 receptors: toward understanding their activation. *Cold Spring Harb Perspect Biology.* 2010, Vol. 2, 12, p. a004010.

**Thorn, C.A., Atallah, H., Howe, M. & Graybiel, A.M. 2010.** Differential dynamics of activity changes in dorsolateral and dorsomedial striatal loops during learning. *Neuron.* 2010, Vol. 66, 5, pp. 781-795.

**Ting, J. & Feng, G. 2011.** Neurobiology of obsessive-compulsive disorder: insights into neural circuitry dysfunction through mouse genetics. *Curr Opin Neurobiol.* 2011, Vol. 21, 6, pp. 842-848.

**Todtenkopf, M.S. et al. 2006.** Brain reward regulated by AMPA receptor subunits in nucleus accumbens shell. *J Neurosci.* 2006, Vol. 26, pp. 11665-11669.

**Toyoda, H, et al. 2007.** Long-term depression requires postsynaptic AMPA GluR2 receptor in adult mouse cingulate cortex. *J Cell Physiol.* 2007, Vol. 211, 2, pp. 336-43.

**Turrigiano, G.G. & Nelson, S.B. 2004.** Homeostatic plasticity in the developing nervous system. *Nat. Rev. Neurosci.* 2004, Vol. 5, pp. 97-107.

**van den Akker, E., et al. 1999.** Targeted inactivation of Hoxb8 affects survival of spinal ganglion and causes aberrant limb reflexes. *Mech Dev.* 1999, Vol. 89, pp. 103-114.

**Ventura, A., Meissner, A., Dillon, C.P., McManus, M., Sharp, P.A., Van Parijs, L., Jaenisch, R. & Jacks, T. 2004.** Cre-lox-regulated conditional RNA interference. *Proc. Natl. Acad. Sci. USA.* 2004, Vol. 101, 28, pp. 10380-10385.

**Vialou, V. et al. 2010.** ΔFosB in brain reward circuits mediates resilience to stress and antidepressant responses. *Nature Neurosci.* 2010, Vol. 13, pp. 745-752.

**Voom, P., et al. 2004.** Putting a spin on the dorsal-ventral divide of the striatum. *Trends Neurosci.* 2004, Vol. 27, 8, pp. 468-474.

**Wallace, D.L., et al. 2008.** The influence of ΔFosB in the nucleus accumbens on natural reward-related behavior. *J. Neurosci.* 2008, Vol. 28, 41, pp. 10272-10277.

**Wan Y., Feng G. & Calakos N. 2011.** Sapap3 deletion causes mGluR5-dependent silencing of AMPAR synapses. *J Neurosci.* 2011, Vol. 31, pp. 16685-16691.

**Wan, Y., et al. 2014.** Circuit-specific striatal dysfunction in the Sapap3-null mouse model of obsessive-compulsive disorder. *Biol. Psychiatry.* 2014, Vol. 75, 8, pp. 623-630.

**Welch, J. et al. 2007.** Cortico-striatal synaptic defects and OCD-like behaviors in Sapap3-mutant mice. *Nature.* 2007, Vol. 448, pp. 894-900.

**Werme, M., Messer, C., Olson, L., Gilden, L., Thoren, P., Nestler, E.J. & Stefan, B. 2002.** ΔFosB regulates wheel running. *J. Neurosci.* 2002, Vol. 22, 18, pp. 8133-8138.

**Wilson, R.C., et al. 2013.** Orbitofrontal cortex as a cognitive map of task space. *Neuron.* 2013, Vol. 81, 2, pp. 267-279.

**Wondolowski, J. & Dickman, D. 2013.** Emerging links between homeostatic synaptic plasticity and neurological disease. *Front. Cell. Neurosci.* 2013, Vol. 7, p. 223.

**Xiong, Q, et al. 2015.** Selective corticostriatal plasticity during acquisition of an auditory discrimination task. *Nature.* 2015, Vol. doi:10.1038/nature14225.

**Yim, Y.Y., et al. 2013.** Slitrks control excitatory and inhibitory synapse formation with LAR receptor protein tyrosine phosphotases. *Proc. Natl. Acad. Sci. USA.* 2013, Vol. 110, 10, pp. 4057-4062.

**Yin, H.H. and Knowlton, B.J. 2006.** The role of the basal ganglia in habit formation. *Nat. Rev. Neurosci.* 2006, Vol. 7, pp. 464-76.

**Yin, H.H., et al. 2004.** Lesions of the dorsolateral striatum preserve outcome expectancy but disrupt habit formation in instrumental learning. *Eur J Neurosci.* 2004, Vol. 19, 1, pp. 181-189.

**—. 2005.** The role of the dorsomedial striatum in instrumental conditioning. *Eur J Neurosci.* 2005, Vol. 22, 2, pp. 513-523.

**Yoshii, A. & Constantine-Paton, M. 2007.** BDNF induces transport of PSD-95 to dendrites through PI3K-AKT signaling after NMDA receptor activation. *Nat Neurosci.* 2007, Vol. 10, pp. 702-711.

**Zhang, J., et al. 2002.** C-fos regulates neuronal excitability and survival. *Nat Genetics.* 2002, Vol. 30, pp. 416-420.

**Zhao, S. et al. 2011.** Cell-type Specific Optogenetic Mice for Dissecting Neural Circuitry Function. *Nat. Methods.* 2011, Vol. 8, 9, pp. 745-752.

**Zheng, C.Y., et al. 2011.** MAGUKs, synaptic development, and synaptic plasticity. *Neuroscientist.* 2011, Vol. 17, pp. 493-512.

**Zhou L., Furuta T. & Kaneko T. 2003.** Chemical organization of projection neurons in the rat accumbens nucleus and olfactory tubercle. *Neuroscience.* 2003, Vol. 120, pp. 783-798.

**Zhou, Y., Takahashi, E., Li, W., Halt, A., Wiltgen, B., Ehninger, D., Li, G.D., Hell, J.W., Kennedy, M.B. & Silva, A.J. 2007.** Interactions between the NR2B Receptor and CaMKII modulate synaptic plasticity and spatial learning. *J. Neurosci.* 2007, Vol. 27, 50, pp. 13843-53.

**Zuchner, S., et al. 2009.** Multiple rare SAPAP3 missense variants in trichotillomania and OCD. *Mol Psychiatry.* 2009, Vol. 14, 1, pp. 6-9.

**—. 2006.** SLITRK1 mutations in trichotillomania. *Mol Psychiatry.* 2006, Vol. 11, 10, pp. 887-9.

# Biography

Louis Yunshou Tee (born June 29th, 1982 in Singapore) is an MD-PhD student who is training to become a clinician-scientist. He obtained his Bachelors of Science with Honors in Biomedical Engineering from Brown University in 2006, and he earned his PhD in Neurobiology from Duke University under the mentorship of Professor Guoping Feng in 2015. He will complete his MD from the Duke-National University of Singapore Graduate Medical School in 2016. He was awarded a MD-PhD scholarship from the Agency for Science, Technology and Research in Singapore, and is a member of Sigma Xi, the scientific research honors society.